ECE 5320

Lecture #9

Nanoparticle vs. Magnetic Properties

Magnetic Anisotropy

$$H_{ex} = -2\sum_{i<j} J_{ij}\vec{S}_i \cdot \vec{S}_j - K\sum_i (S_{zi})^2$$

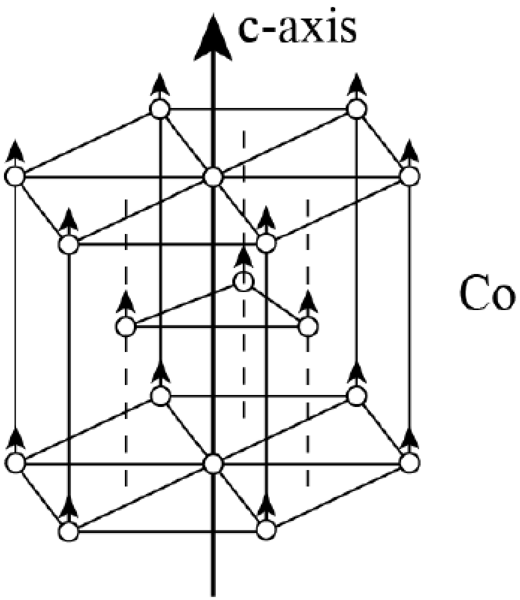

Uniaxial Magnetic Anisotropy

Anisotropy Field $$H_{an} = \frac{2K}{\mu_0 M_s}$$

Bulk Co in its demagnetized, multi-domain state

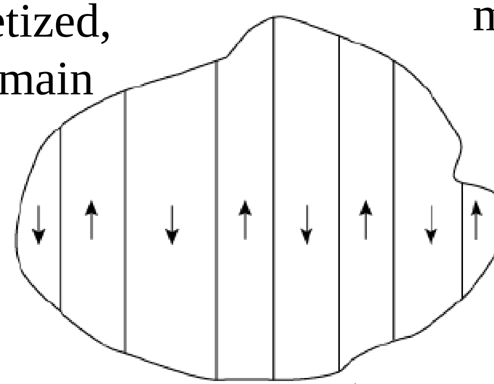

Minimization of magnetostatic energy

$$U_B = \frac{1}{2\mu_0}\int_{allspace} B^2 d\tau$$

leads to domain wall formation

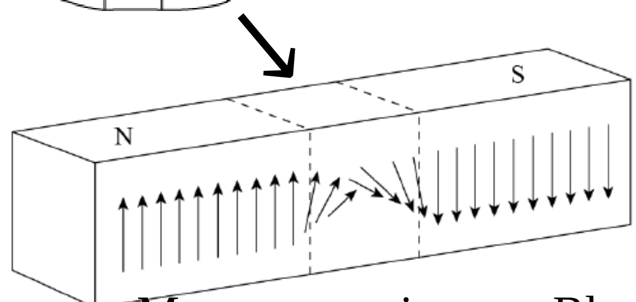

Moment rotation at a Bloch Wall

Exchange energy per unit area of Bloch wall $\sigma_{BW} = \pi\sqrt{AK}$ where $A = \dfrac{2J_{ex}S^2}{a}$

for a simple cubic lattice with lattice constant a.

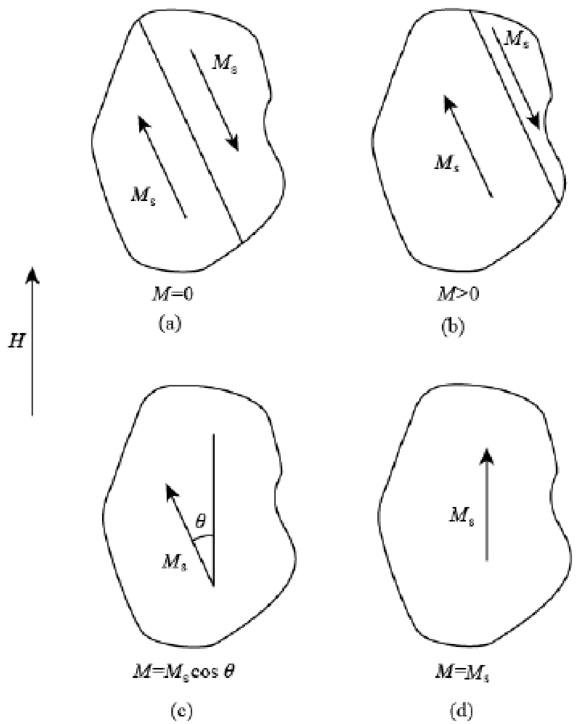

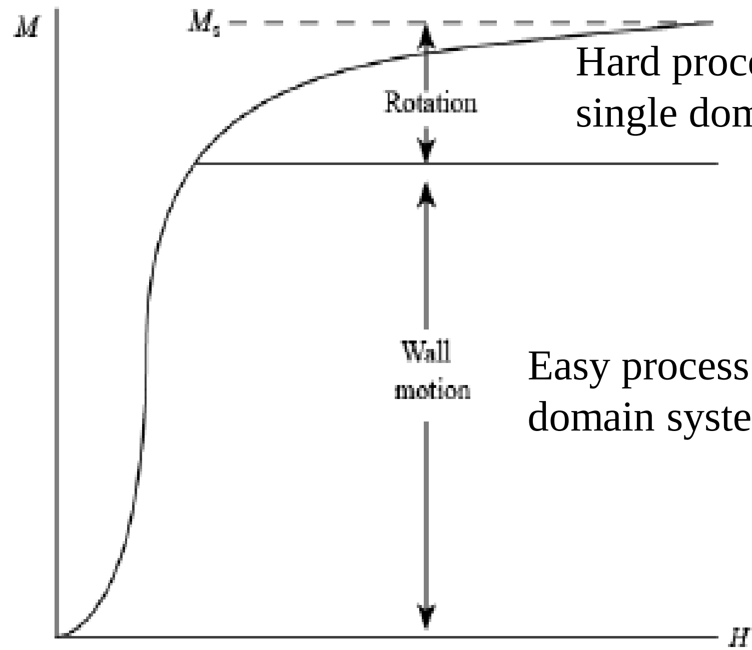

Hard process in a single domain system

Easy process in a multi-domain system

Hysteresis Loop

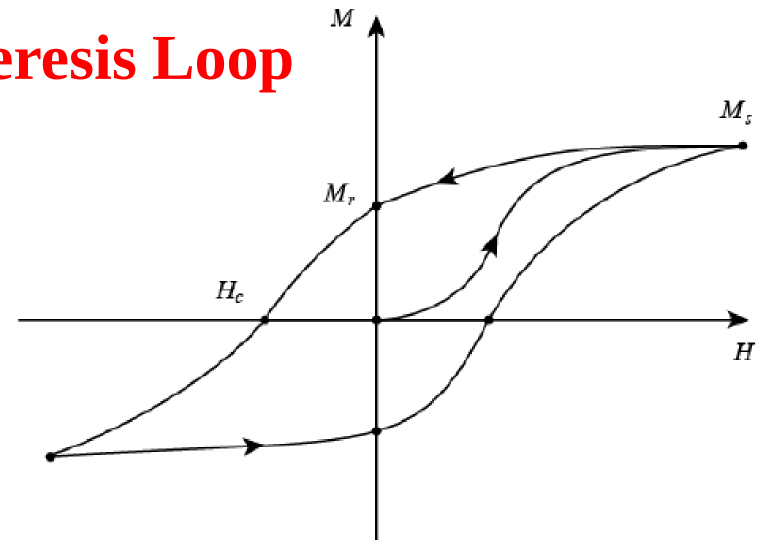

The hysteresis loop defines the technological properties of the magnetic material

M_s = Saturation Magnetization

M_r = Remnant Magnetization

H_c = Coercivity

Critical Size for SMD Particles

Magnetostatic *vs.* wall energy as a function of particle size for a spherical particle of radius *r*

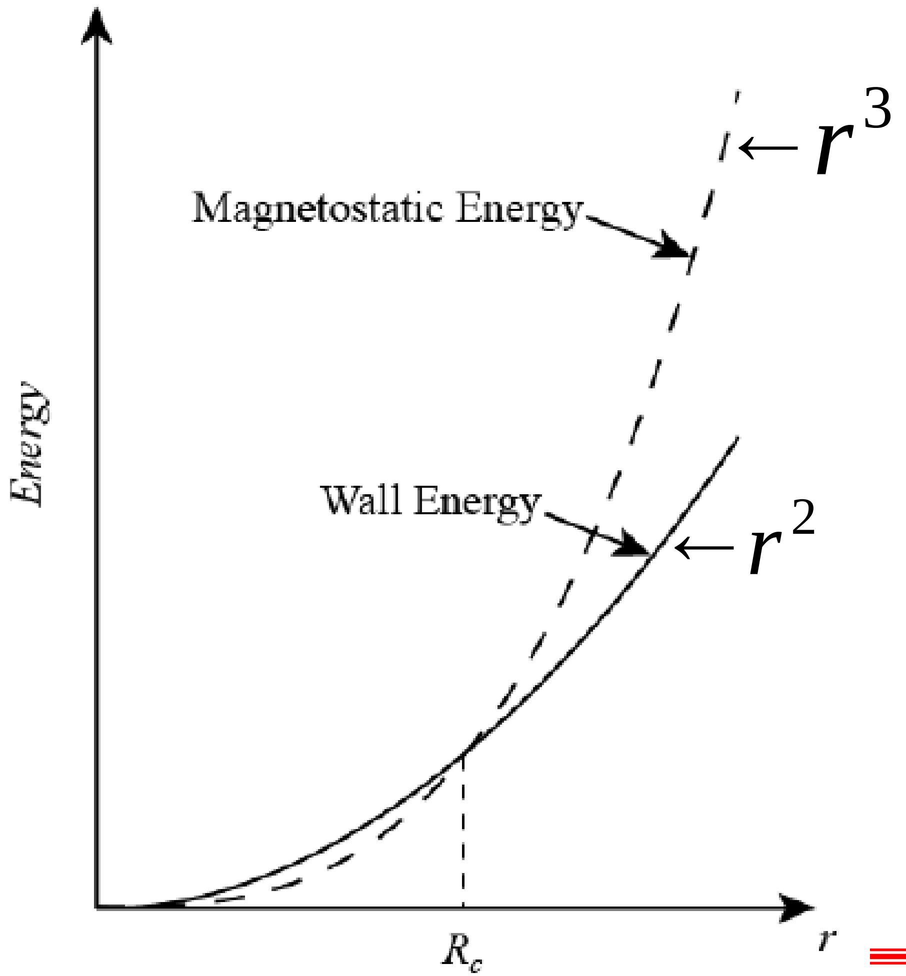

$$R_C = R_{SMD} = \frac{6\sqrt{AK}}{\mu_0 M_s^2}$$

Below $R_\mathbf{c}$ the particle is a Single Magnetic Domain, and thus permanently magnetized. The demagnetized state cannot be formed.

$R_\mathbf{c} \sim 100$ nm

Coercivity as a function of particle size

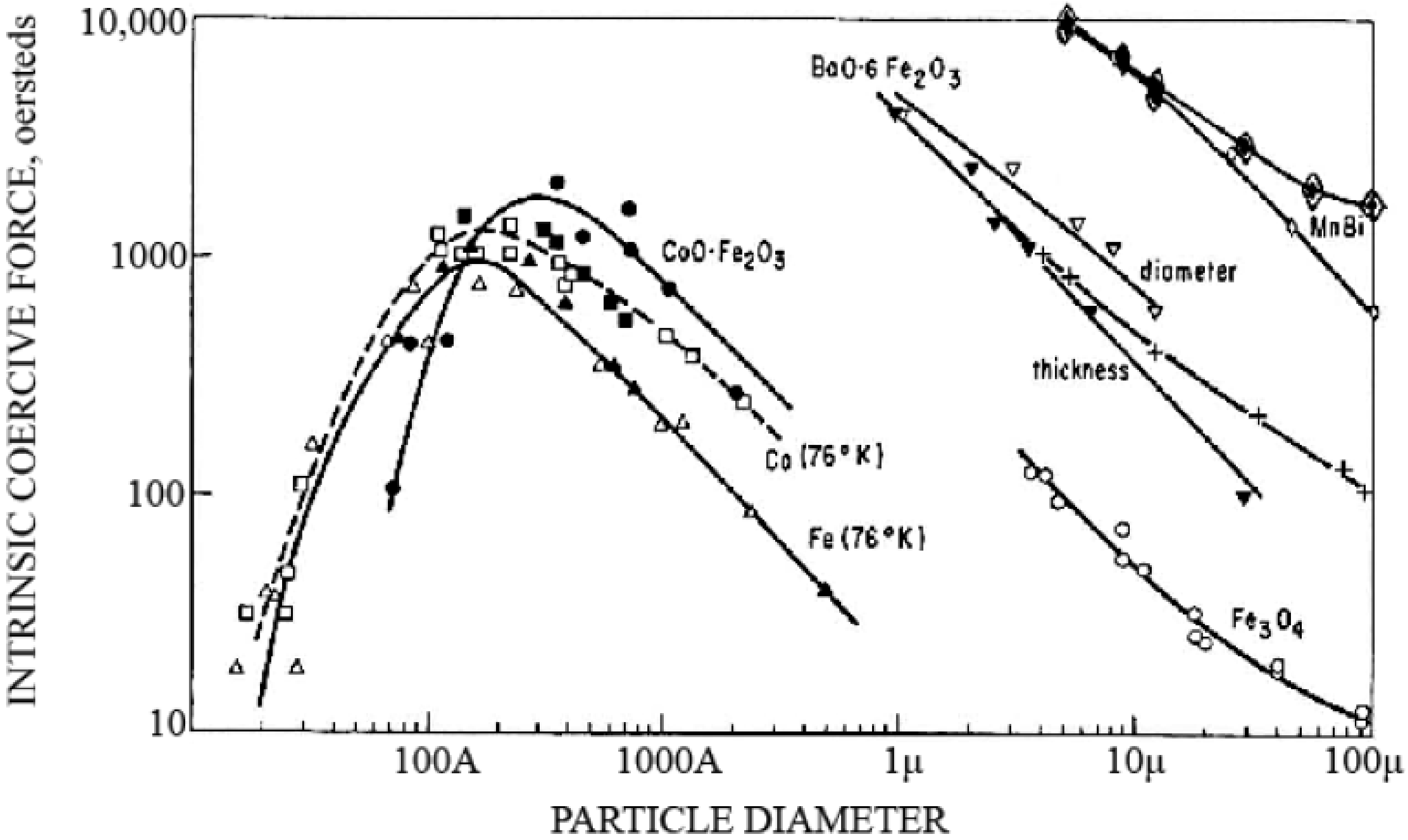

F. E. Luborsky J. Appl. Phys.32 (1961) S171

Nanomagnetism: Coercivities and Spin Reversal Mechanisms

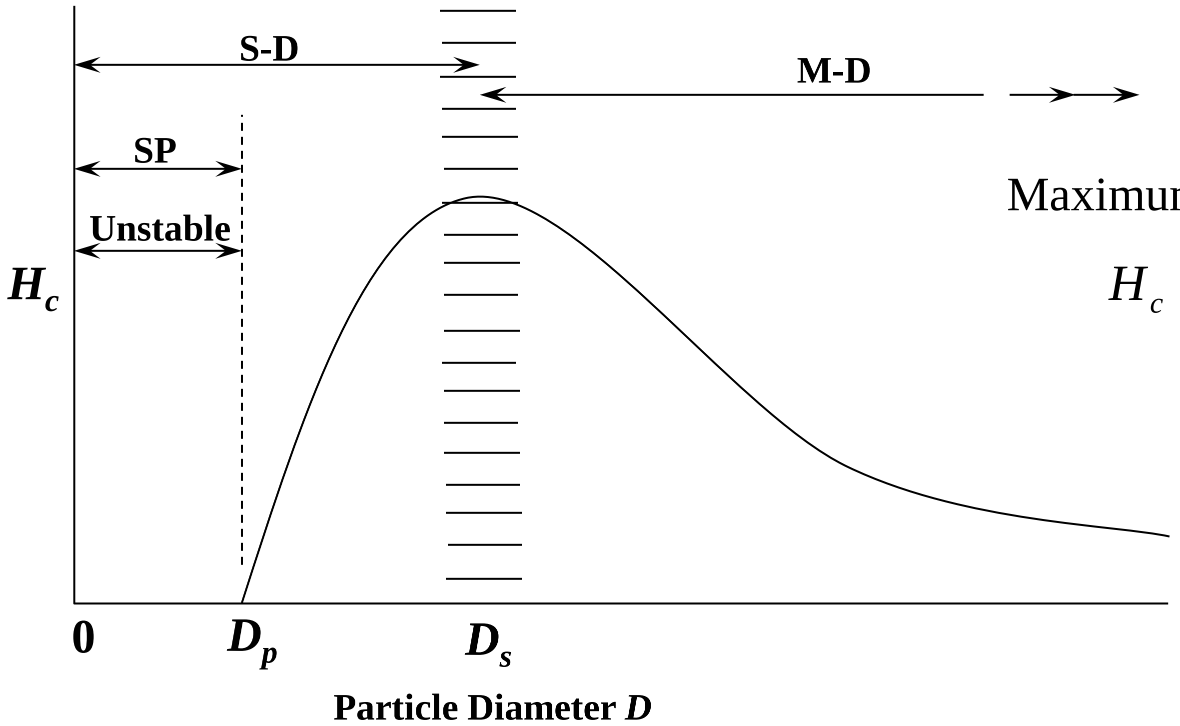

Maximum coercivity

$$H_c = \frac{2K}{\mu_0 M_s}$$

Single-magnetic domain particle
Coherent spin rotation

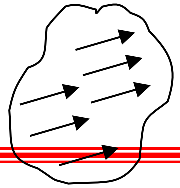

Nanoparticle

$K \sim 10^5$ J/m^3

Multi-magnetic domain structure
Magnetic wall movement

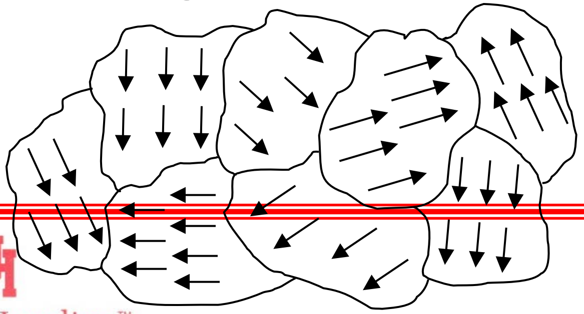

Bulk

$K \sim 10^3$ J/m^3

Origin of magnetic anisotropy enhancement in nanoparticles

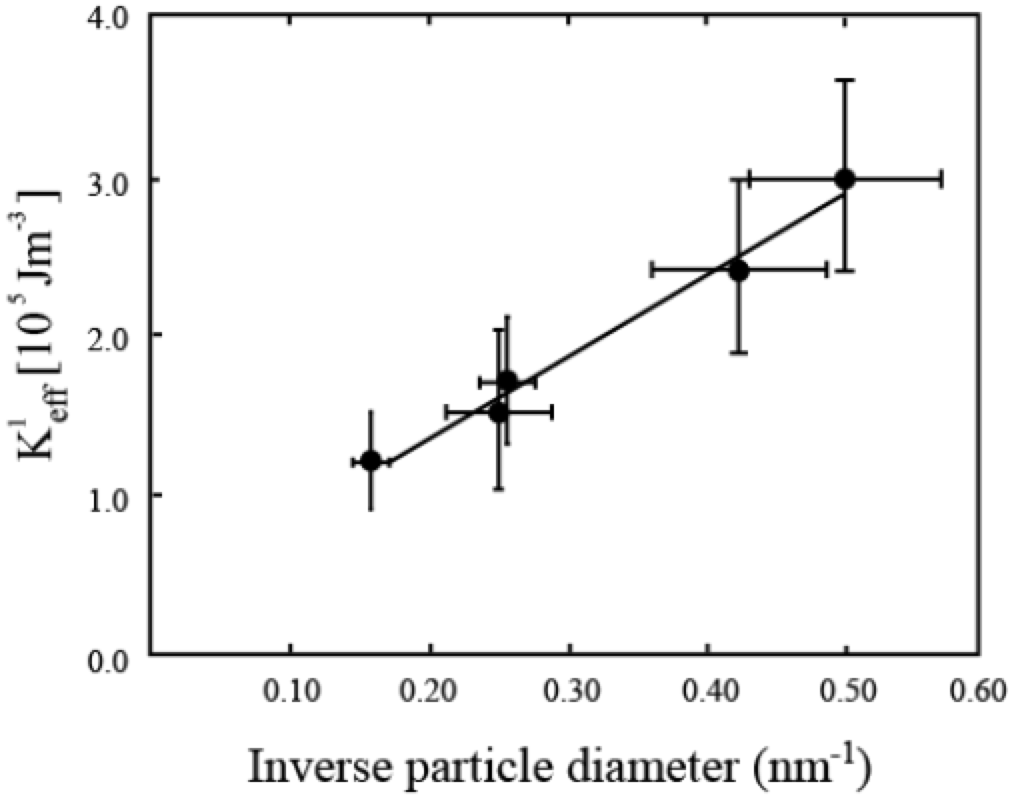

F. Bødker, S. Mørup, S. Lideroth, Phys. Rev. Lett. 72 (1994) 282

$$K_{eff} = K_c + \frac{6K_s^{'}}{D}$$

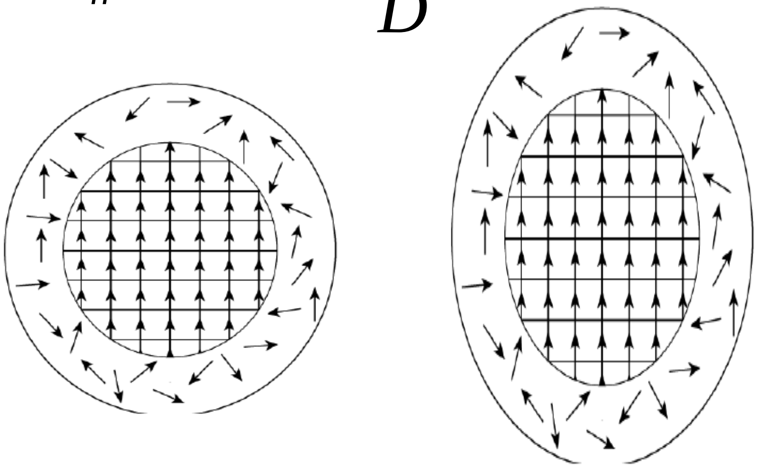

$$K_{eff} = K_c + K_s + K_\sigma + K_{sh}$$

c = core
s = surface
σ = stress
sh = shape

Nanoparticle coercivity for coherent spin rotation (Stoner and Wohlfarth model)

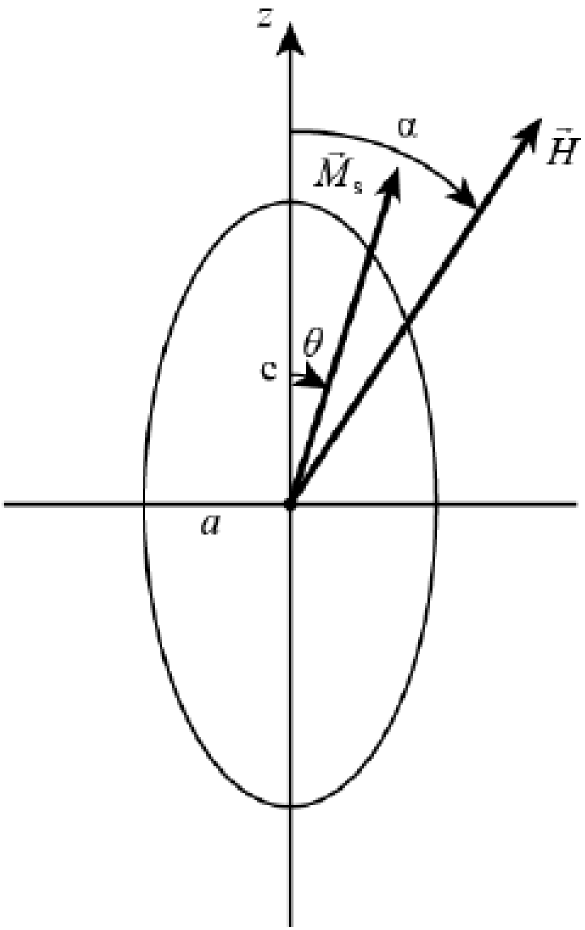

Easy axis
(axis of revolution)

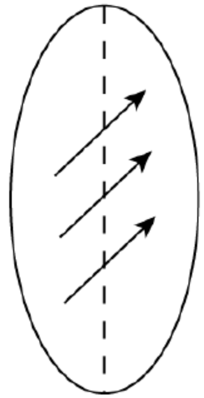

coherent
moment
rotation

Maximum coercivity for coherent spin rotation of a single magnetic domain particle with uniaxial total effective anisotropy

$$H_c = \frac{2K_u}{\mu_0 M_s}$$

E.C. Stoner, E.P. Wohlfarth, Trans. Roy. Soc. Lond. A 240 (1948) 599

Spin Dynamics in Magnetic Nanoparticles

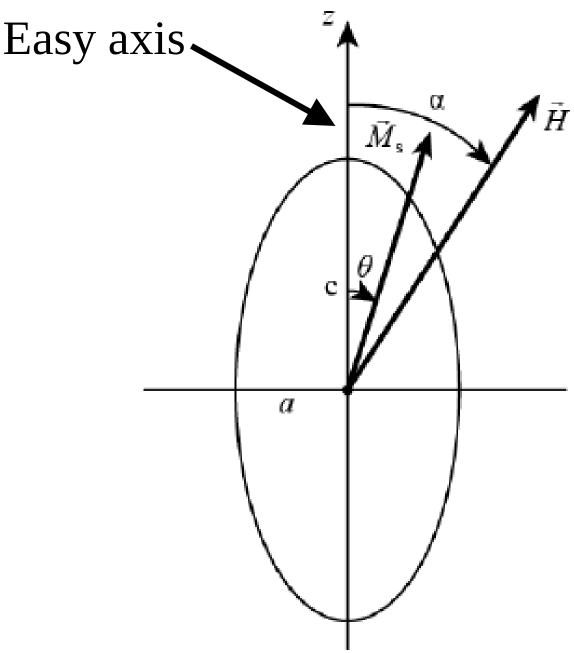

$$E_a(\theta) = K_u V \sin^2 \theta$$

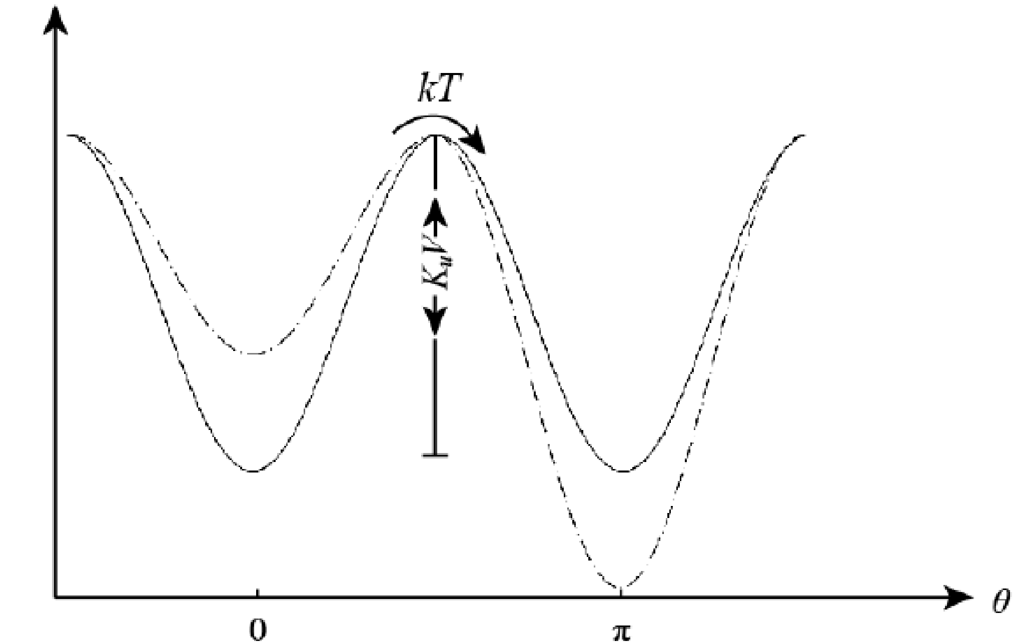

Temperature dependence of coercivity

$$H_c = \frac{2K_u}{\mu_0 M_s}\left[1 - \left(\frac{25kT}{K_u V}\right)^{1/2}\right]$$

(thermally assisted spin reversals)

Superparamagnetic relaxation time

$$\tau = \tau_0 \exp\left(\frac{K_u V}{kT}\right)$$

Due to fast moment reversals at elevated temperatures the internal magnetic order of the particle escapes detection. You must either lower the temperature or use ultrafast measuring techniques that can record the moment before it flips.

Superparamagnetism of Small Magnetic Particles

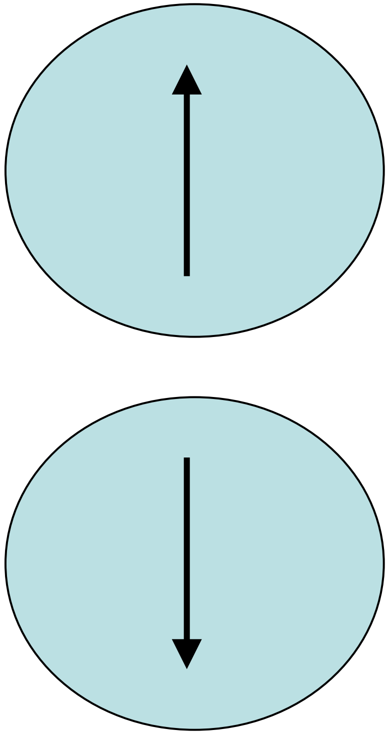

Energy barrier
$\Delta E = K_u V$

where Ku is the effective uniaxial magnetic anisotropy Energy density and V is the particle volume

Relaxation Time

$t_{RELAX} = t_0 \exp(K_u V/kT)$

Magnetocrystalline Anisotropy

Shape Anisotropy

Surface effects

Observe net magnetic moment when
$t_{MEAS} < t_{RELAX}$

Micro-magnetics and Spin Dynamics

-**Mössbauer spectroscopic measurements**

Probe local magnetic moments and internal magnetic fields, with a response time of

$$\tau_m = \tau_{Möss} = 10\ ns$$

-DC Magnetization measurements

Probe global magnetic properties in an applied field, with a response time of

$$\tau_m = \tau_{SQUID} = 10\ s$$

Hysteresis Loops for $CoFe_2O_4$ Block Copolymers

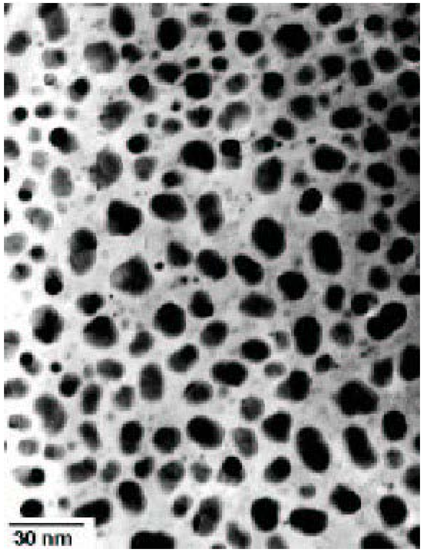

Hysteresis due to particle moment rotation away from the particle's easy axis to the direction of the applied magnetic field.

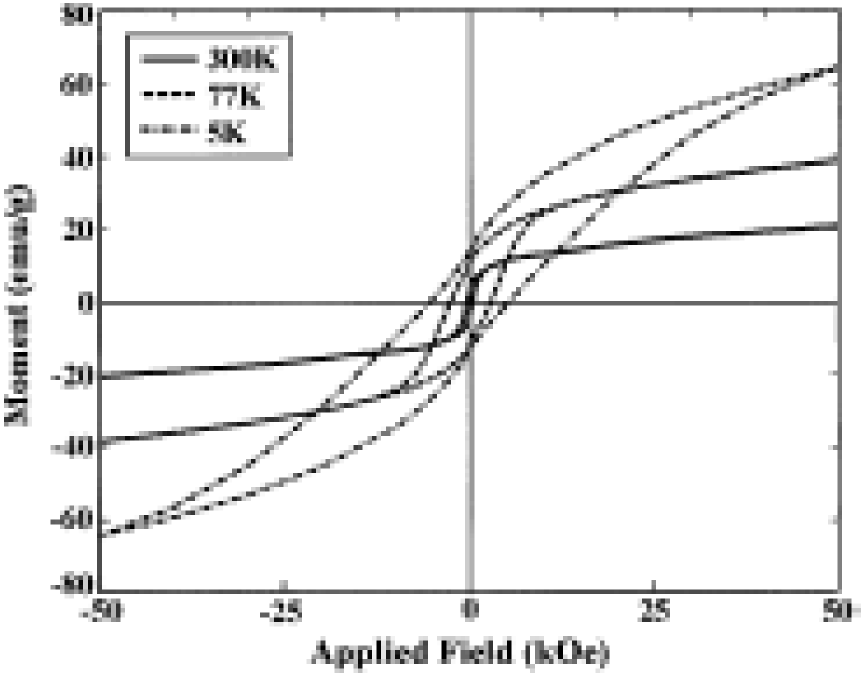

The temperature at which the coercivity vanishes defines the blocking temperature $\boldsymbol{T_B}$ for SQUID magnetometry.

Ahmed, Ogal, Papaefthymiou, Ramesh and Kofinas, Appl. Phys. Letts 80 (2002) 1616

Modeling Dynamical Spin Fluctuations in Isolated Nanostructures

Determination of Blocking Temperature

Experimentally the temperature at which the Mössbauer spectra pass from magnetic, six-line spectra to paramagnetic or quadrupolar, two-line spectra defines T_B for Mössbauer

Theoretically T_B is defined by:

$$\tau_m = \tau_0 \exp\left(\frac{K_u V}{k T_B}\right) \quad \rightarrow \quad T_B = \frac{K_u V}{k \ell n(\tau_m / \tau_0)}$$

Spectrum Key

Magenta: spectral signature of magnetic particle core (internal iron sites)

Green: spectral signature of surface layers (surface iron sites)

G. C. Papaefthymiou, Biochim. Biophys. Acta 1800 (2010) 886

Mössbauer spectra of lyophilized, *in vitro* reconstituted HoSF ferritin.

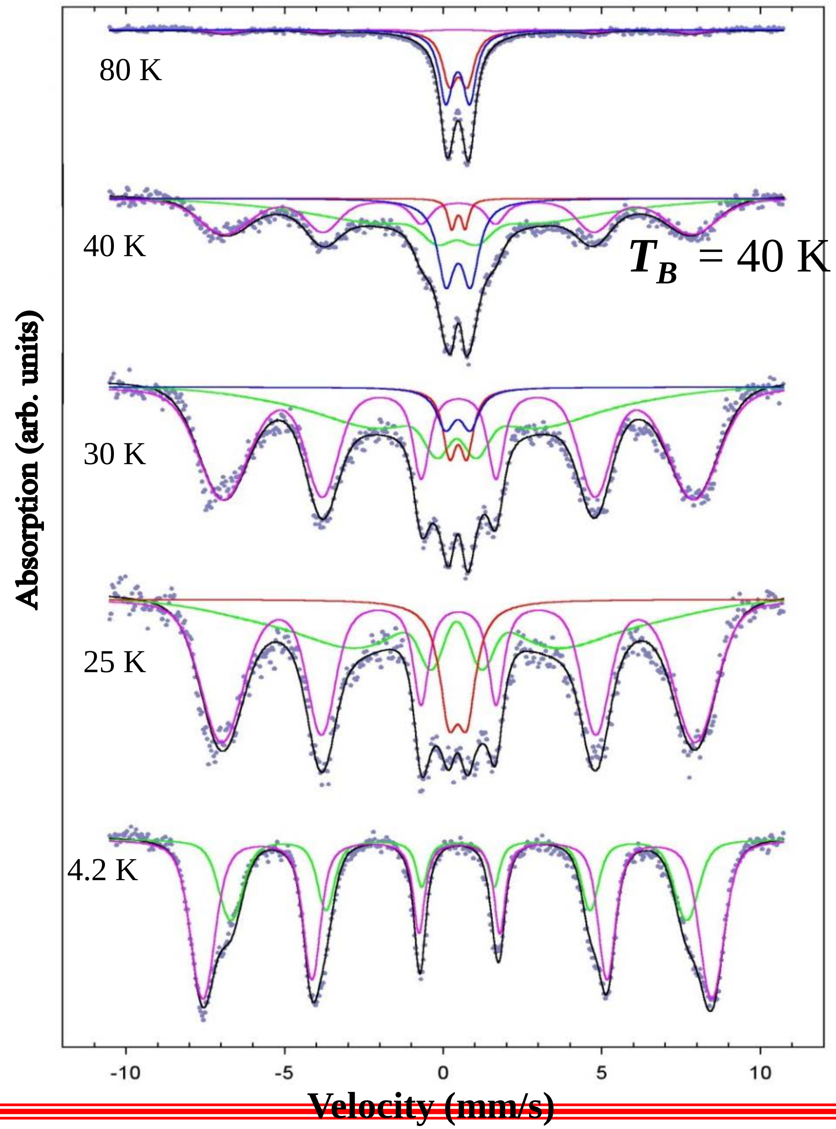

G. C. Papaefthymiou, *et. al. MRS Symp. Proc.* 2007

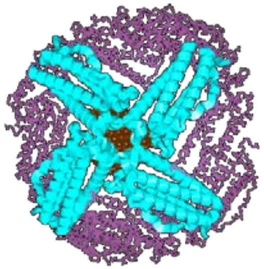

25-nm thick protein shell

Zero-field cooled and field-cooled magnetization of lyophilized HoSF ferritin

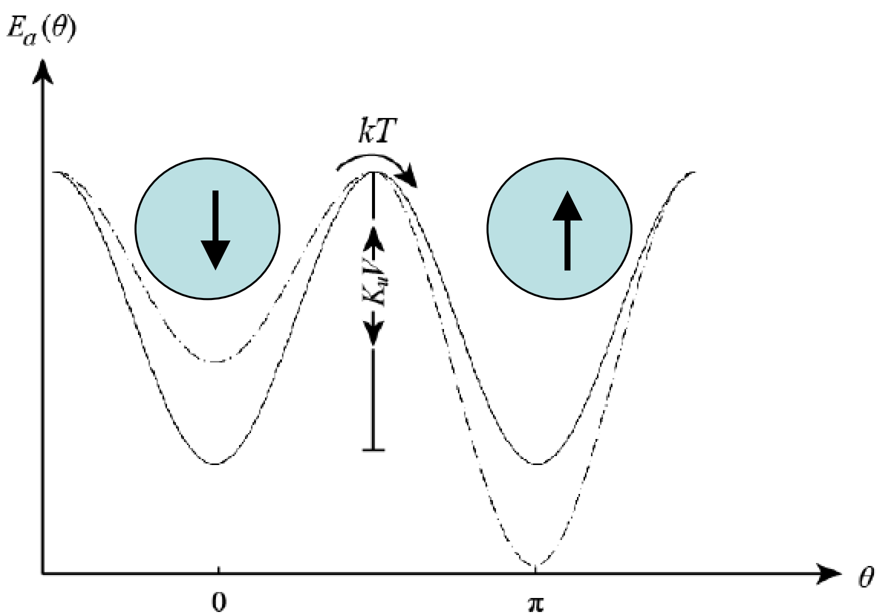

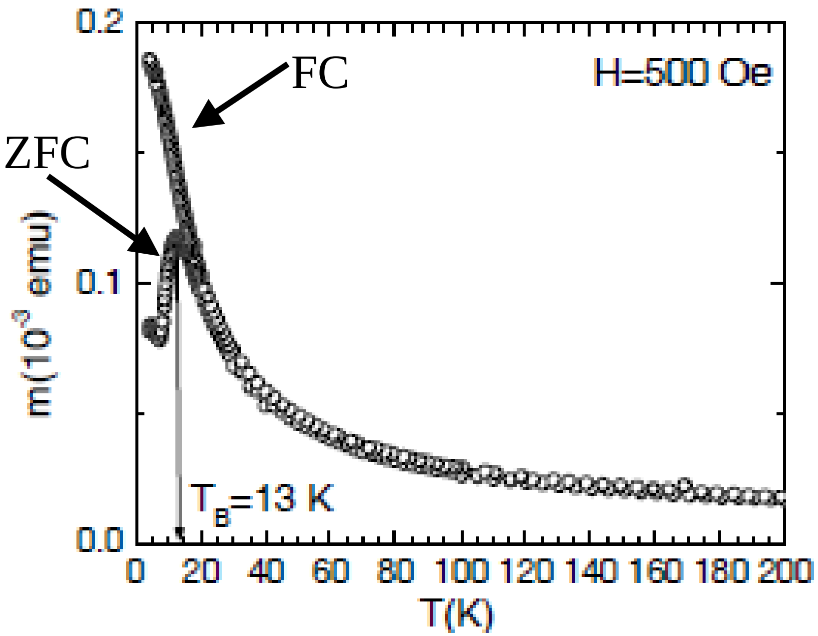

Typical ZFC/FC behavior of an ensemble of magnetically isolated superparamagnetic particles

Note: Saturation magnetization is ~ 0.05 emu/g, weakly magnetic.

Determination of K_u for an ensemble of superparamagnetic nanoparticles

$$\tau = \tau_0 \exp\left(\frac{K_u \langle V \rangle}{kT}\right) \longrightarrow \tau_m = \tau_0 \exp\left(\frac{K_u \langle V \rangle}{kT_B}\right)$$

1. Determine average particle volume $<V>$ by TEM
2. Determine T_B with two different techniques, whose measuring response times lie in different time windows
3. Use the Arrhenius equation above to determine τ_0 and K_u

Surface Effects:Temperature Dependence of Mössbauer Magnetic Hyperfine Fields

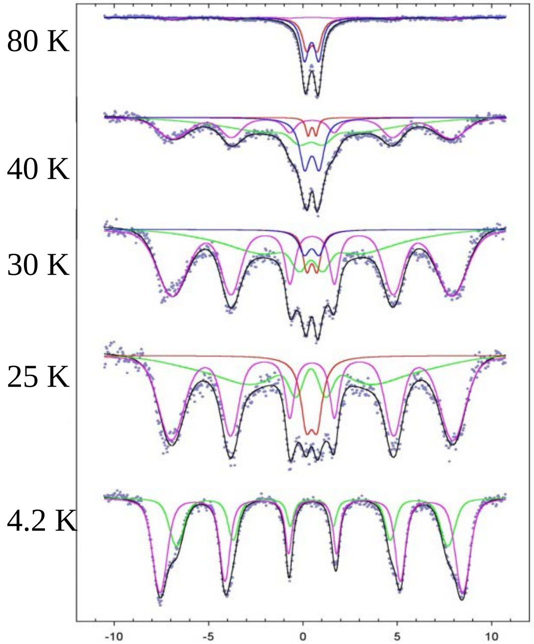

Velocity (mm/s)

Collective magnetic excitations below $\boldsymbol{T_B}$

$$H_{hf}(T) = H_{hf}^{0}\left(1 - \frac{kT}{2K_{eff}V}\right)$$

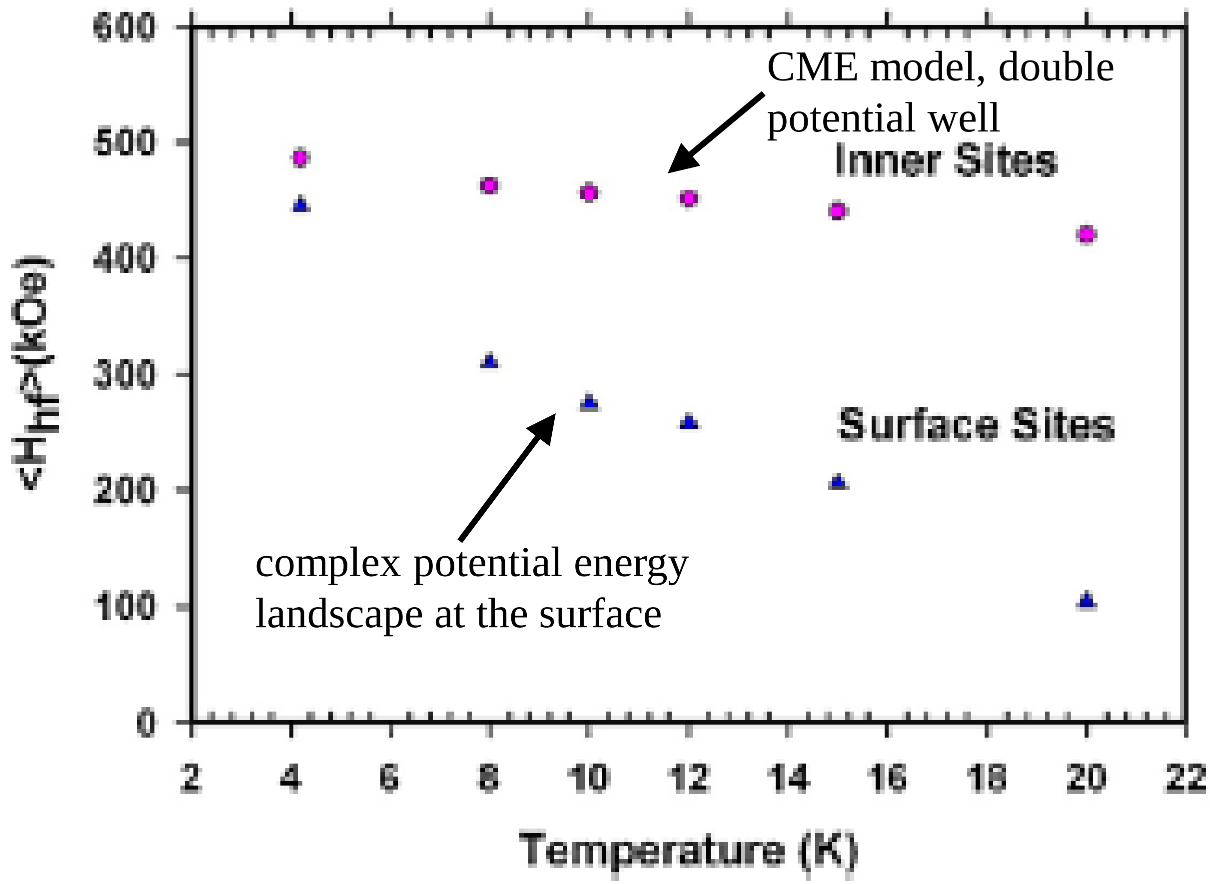

S. Mørup and H. Topsøe, Appl. Phys. 11 (1976) 63

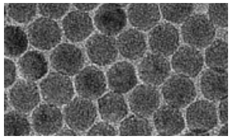

Mössbauer Spectra of γ-Fe_2O_3/Solid Silica Nanoarchitectures

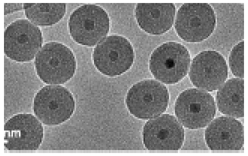

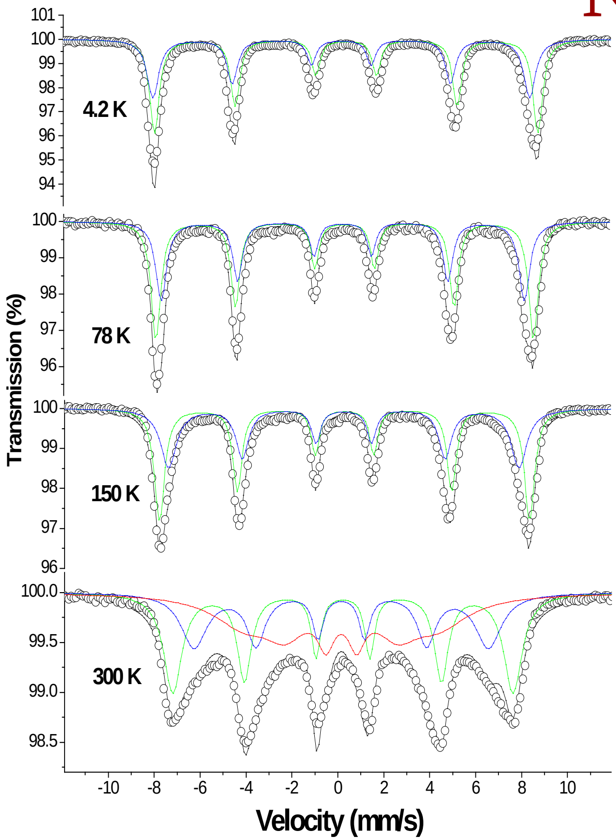

Bare 12 nm particles

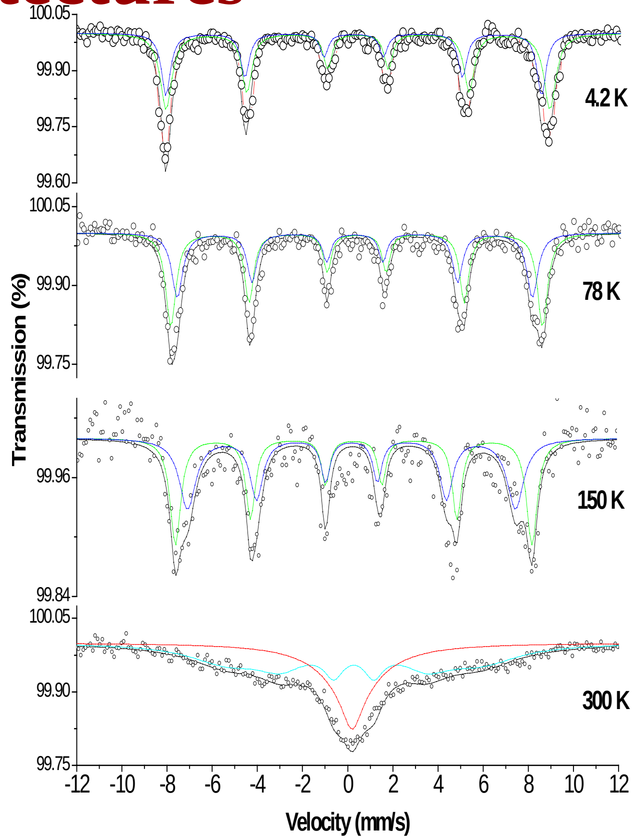

12 nm particles with 25 nm SiO_2 shell

Spectral Key: Blue A-sites, **Green** B-sites of spinel structure

G.C. Papaefthymiou et. al. Phys. Rev. B 80 (2009) 024406

Effect of silica shell on the RT Mössbauer Spectra

Behavior typical of strongly interacting particles

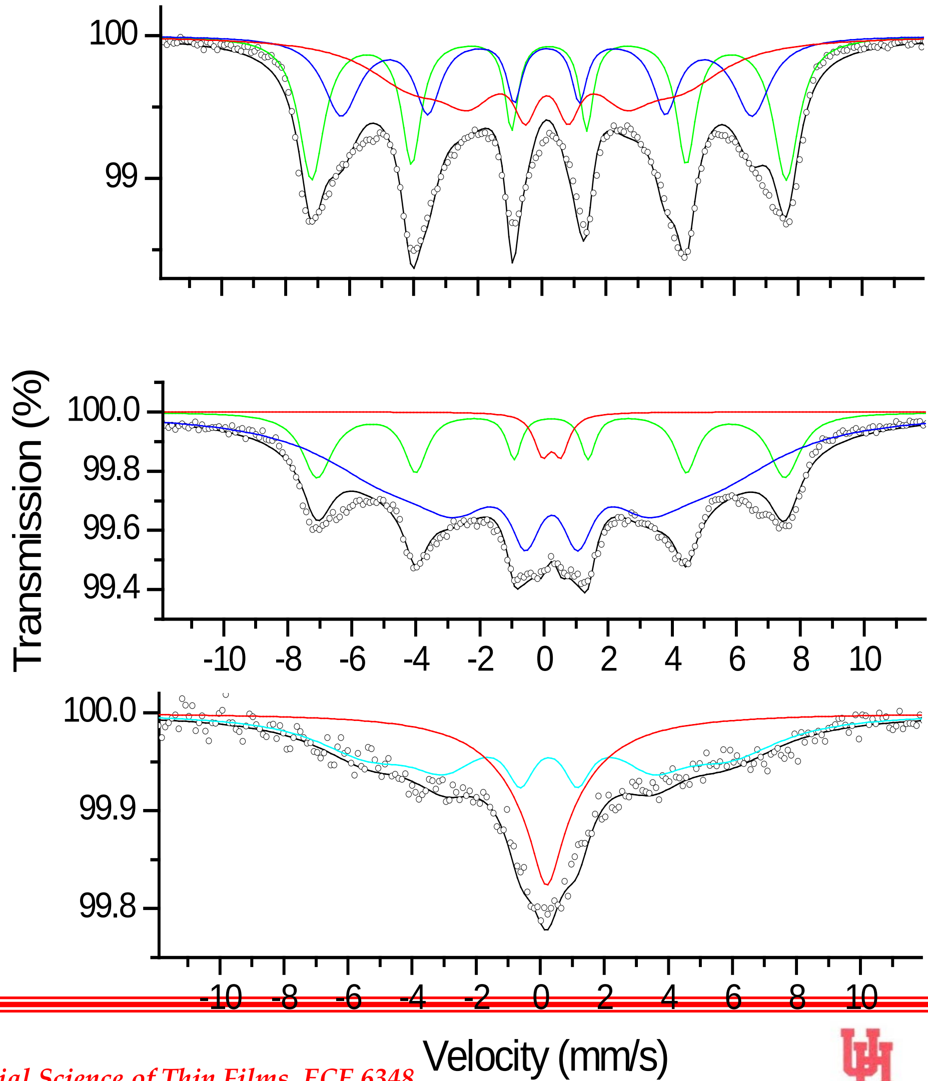

Bare γ-Fe_2O_3 nanoparticles

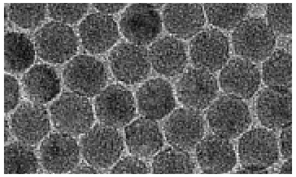

γ-Fe_2O_3 nanoparticles with 4 nm silica shell

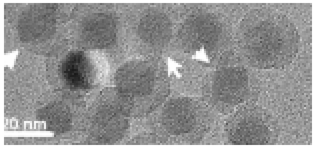

γ-Fe_2O_3 nanoparticles with 25 nm silica shell

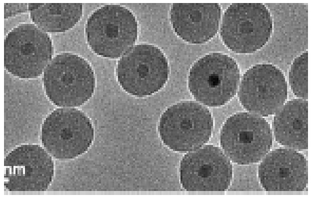

G.C. Papaefthymiou et. al. Phys. Rev. B 80 (2009) 024406

Magnetization of γ-Fe_2O_3/Solid Silica/Mesoporous Silica Nanoarchitectures

A-bare *

B-4 nm (S)

C-25 nm (S)

D-25 nm (S) + 10 nm (MS)

E-25 nm (S) +21 nm (MS)

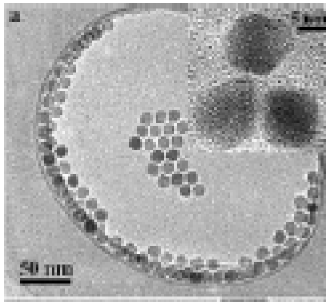

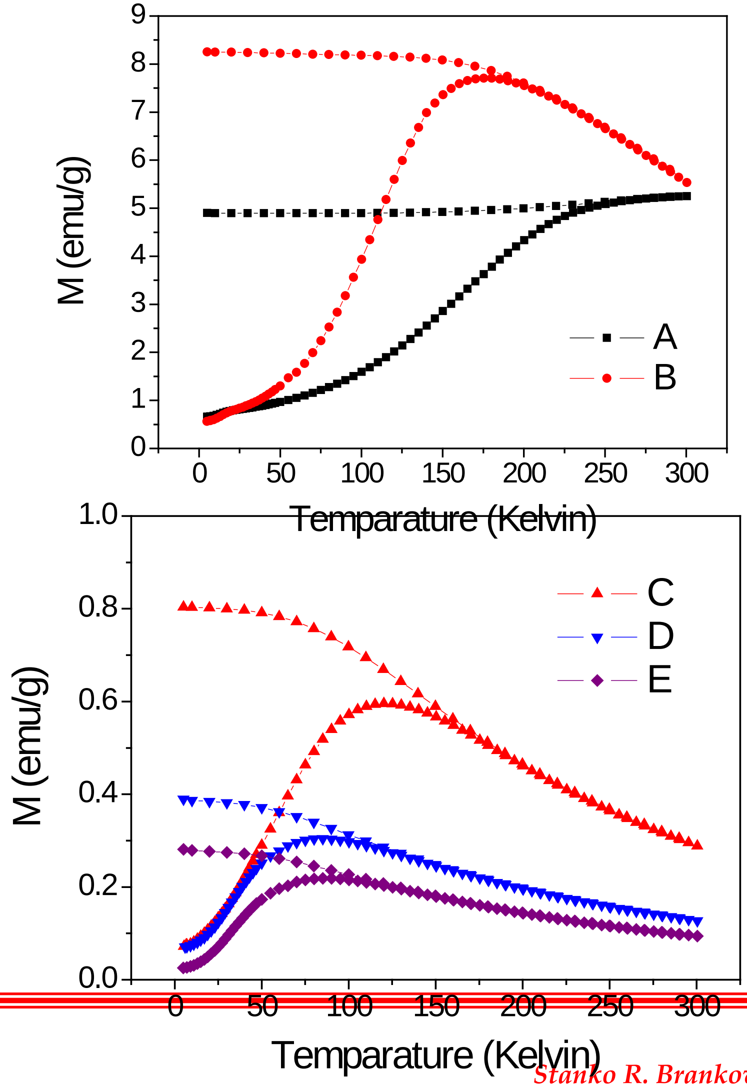

Typical behavior of strongly interacting magnetic nanoparticles, spin-glass-like systems.

* Bare particles are covered with a very thin layer (~1 nm) of oleic acid. Saturation magnetization of the order of ~ 8 emu/g, strongly magnetic

Conclusion

Ferrihydrite is an ***antiferro***-magnet. Magnetization of ferritin is due to uncompensated spins at the surface → Weak magnetism. Protein coat of only 2.5 nm thickness sufficient to magnetically isolate the ferritin iron cores

Maghemite is a ***ferri*** -magnet due to uncompensated spin sublattices in its spinel structure. In small particles uncompensated spins at the surface also contribute → Strong magnetism. Silica coat of 23 nm thickness insufficient to isolate the γ-Fe_2O_3 cores

$$\text{Dipole-dipole interaction} \sim \frac{\vec{\mu}_1 \cdot \vec{\mu}_2}{r^3}$$

Heat Assisted Magnetic Recording Media - Topics

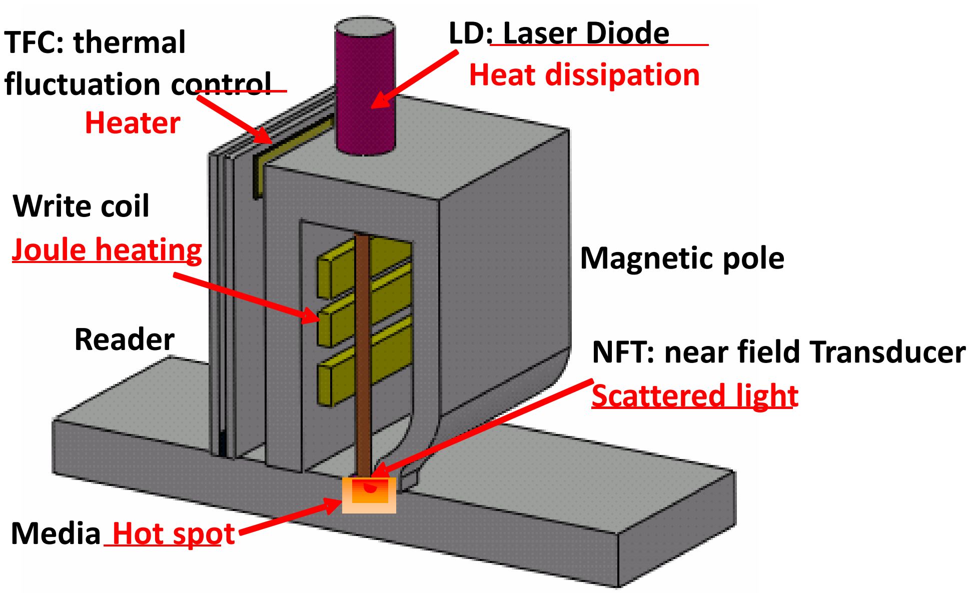

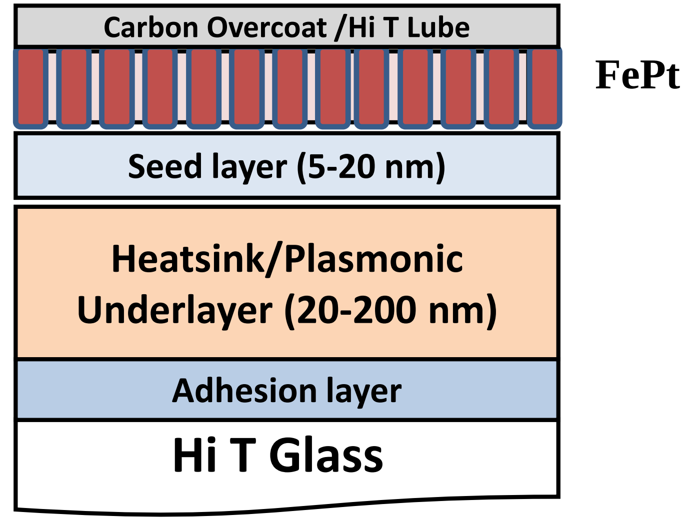

Introduction

- Magnetic Recording Media background and areal density projections

Chemically ordered $L1_0$ FePt media

- Key media parameters and requirements
- Microstructure
- Magnetics
- Status and ongoing efforts

Summary

Seagate HAMR Demo

Dr. Steve Hwang, Vice President Media R&D,
Seagate Technology, RMO Fremont

1007 Gbpsi (1975 kbpi x 510 ktpi)

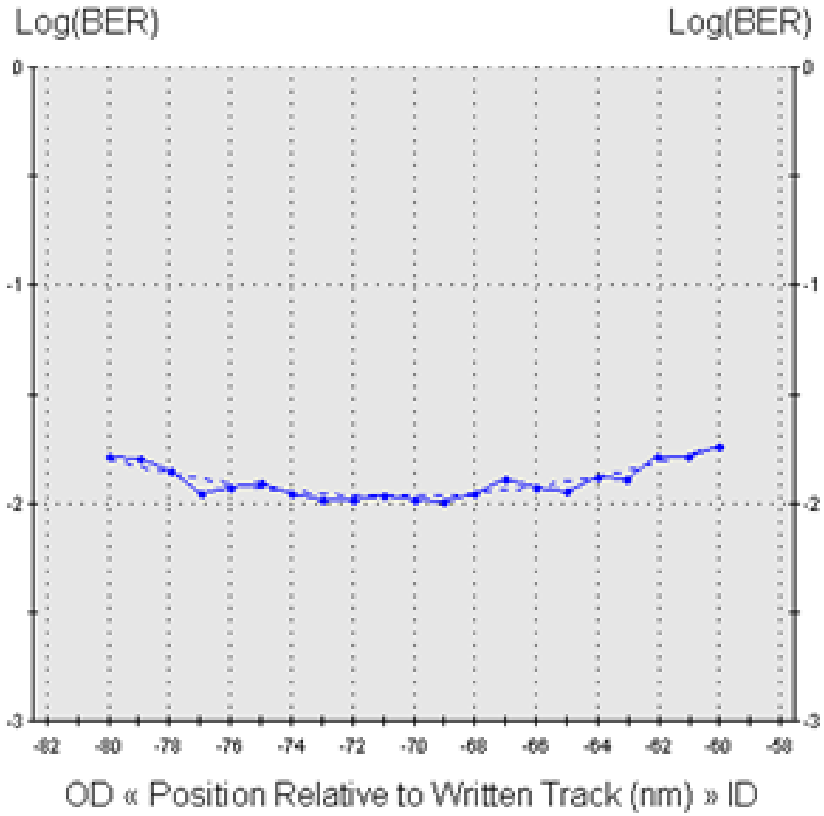

OTC = 0 nm
RWO = -70.72 nm
Log(BER) = -1.99
Squeeze = 0 %TP
OTC Threshold = -2
Curve Fit = Quadratic

LD = 1975.0 KBPI
TD = 510.0 KTPI
AD = 1007.3 Gb/in²

Data Rate = 833.9 Mb/s
RPM = 4200; Sectors = 16
Radius = 24.384 mm; Skew = 0.00°
TD = 510.0 KTPI; TP = 49.8 nm
Iw = 61.0 mA bp; Bias = 0.350 mA
Code: SID formatted

Demo Criteria

- Adjacent tracks written both sides at track pitch with the same laser power and pattern as data track
- On-track bit error rate = $10^{-2.0}$ with no correction/iterations

Limiting factors

- Head Media Spacing
  - much larger than state-of-the-art PMR
  - media roughness, coating thickness, head thermo-mechanical, and clearance management
- Media Distributions
  - distributions much larger than PMR
  - large effective gradient helps
- Electronic Noise
  Lower Mrt and high HMS

] A. Q. Wu, Y. Kubota, T. Klemmer, T. Rausch, C. Peng , Y. Peng, D. Karns, X. Zhu, Y. Ding, E. KC Chang, Y. Zhao, H. Zhou, K. Gao, J.-U. Thiele, M. Seigler, G. Ju, and E. Gage," HAMR Areal Density Demonstration of 1+ Tbpsi on Spinstand", IEEE Trans Mag. 49, 779 (2013)

Successful 2012-2013 for HAMR

<2012>

In March Seagate announced a 1.0 TBPSI demonstration of HAMR on spin stand

Later in October, TDK announced a 1.5 TBPSI demonstrated on spin stand

Seagate CEO ran his annual investor relations talk off a HAMR drive in September

<2013>

October 2013, Japan
Argus HAMR drives were demonstrated in a Win7 computer at CEATEC 2013 Japan

Nov. 2013, Ninbo China
WD demonstrated HAMR enabled 2.5" drive

HAMR Drive Demonstration - CEATEC

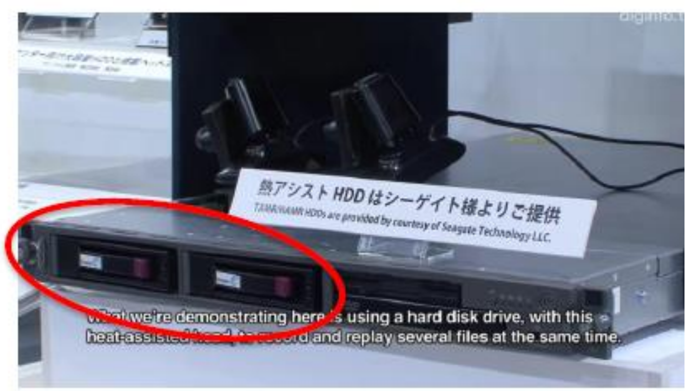

http://www.youtube.com/watch?v=5BYHBV2PTx4

Ultimate Areal Density – HAMR + BPM

Mark H Kryder IEEE Houston, 03-08 updated by Steve Hwang 2012

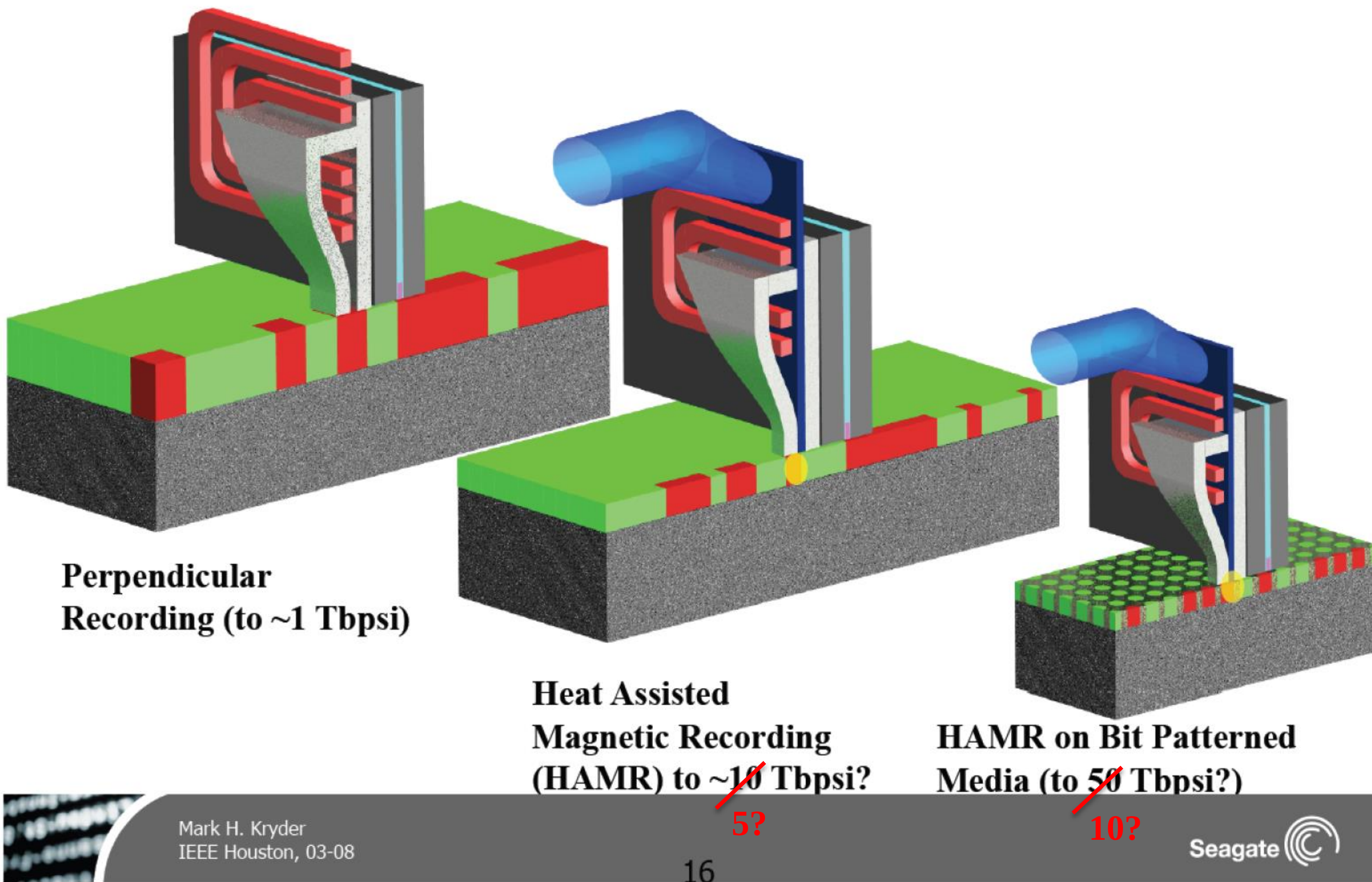

Nanostructured Disks Suppress Noise

Issue: Smaller grains require higher fields to write & maintain thermal stability

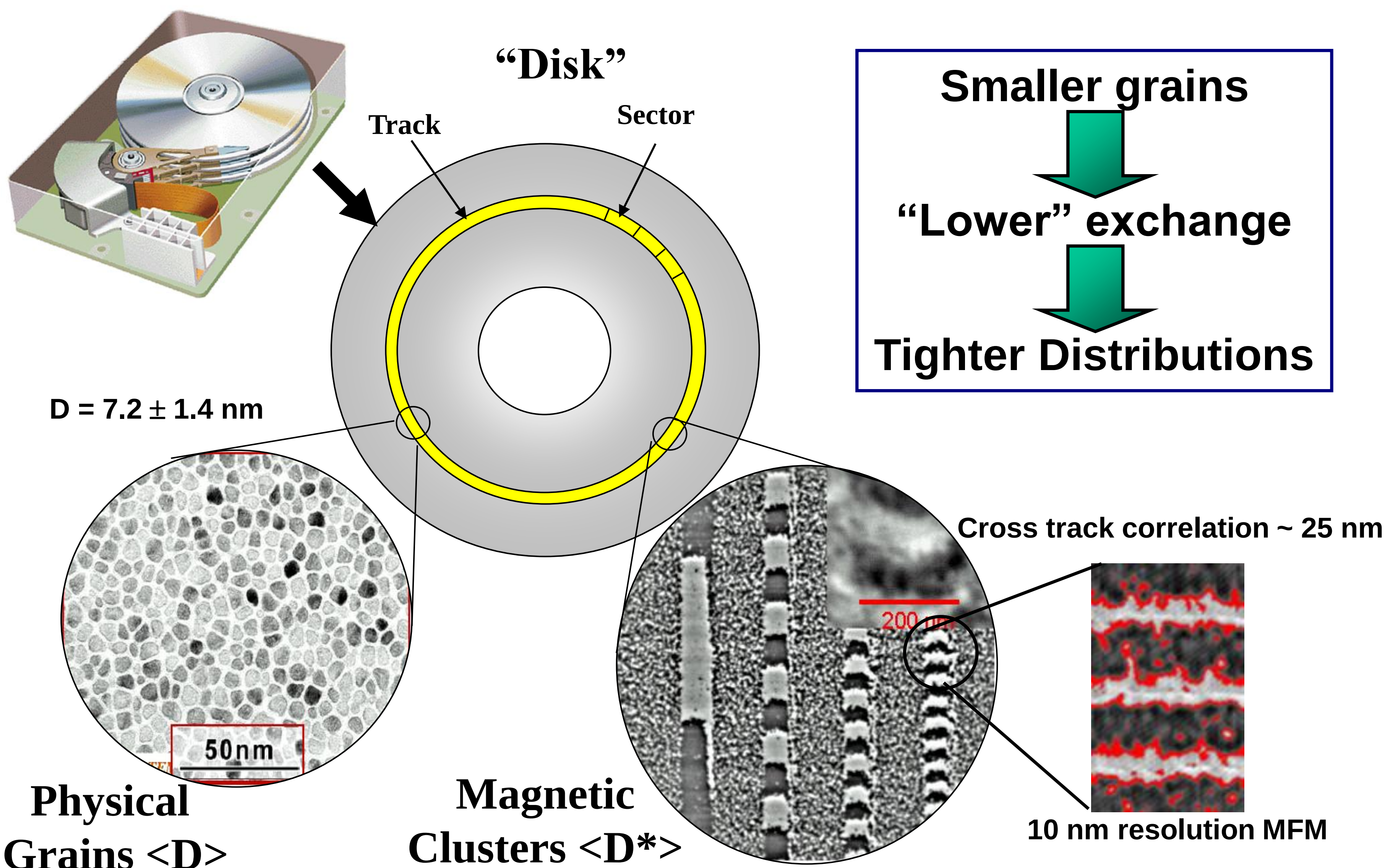

Seagate 2004 J. Ahner, D. Weller

Key Elements of HAMR Media Design

Good Microstructure

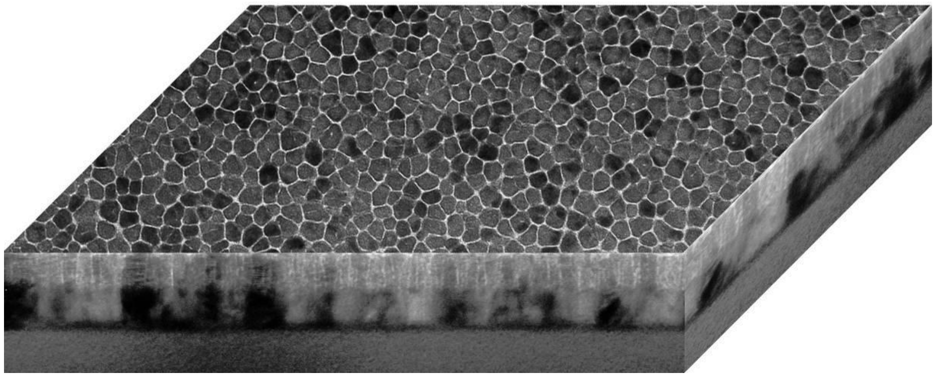

Well Defined Thermal Profile

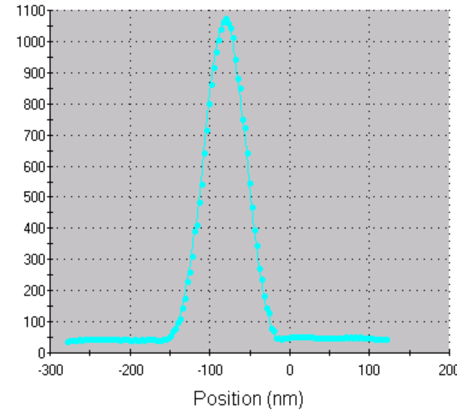

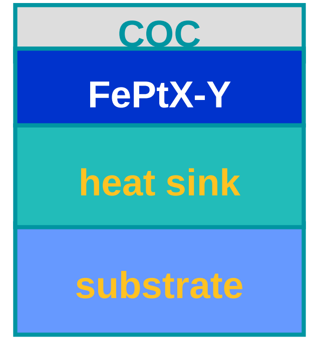

Good Texture and Ordering

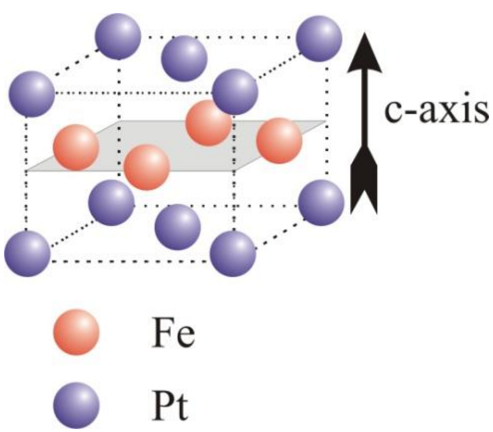

compared to CoCrPt alloys used in PMR FePt $L1_0$ materials used for HAMR media offer

- higher anisotropy
  $\Rightarrow$ larger stability
- lower T_C
- larger dH_K/dT
- tunable by doping, e.g, with Ni or Cu

Magnetics & Distributions

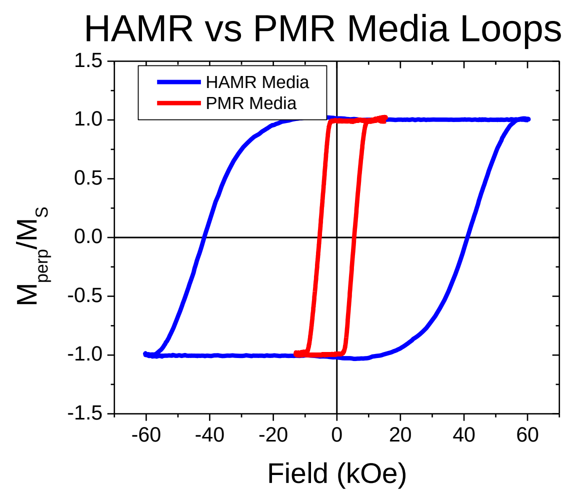

Media Design Constraints – “Trilemma”

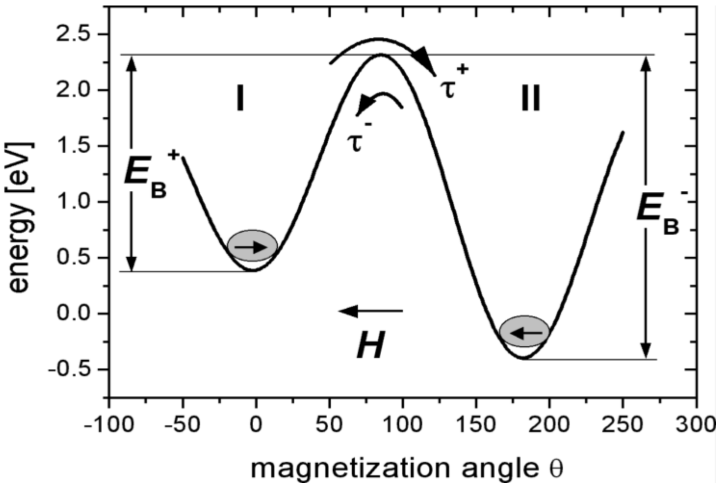

Media SNR

SNR~$\log_{10}(N)$

Small Grains (V)

We are now down to 6-10 grains per bit !

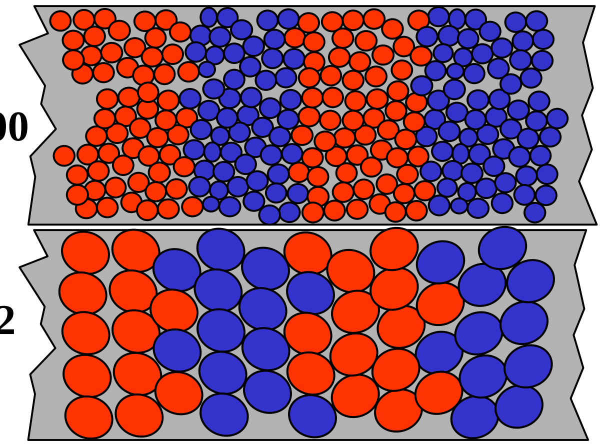

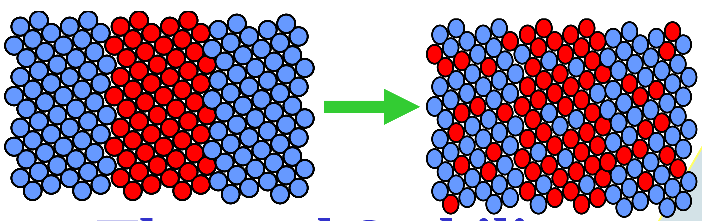

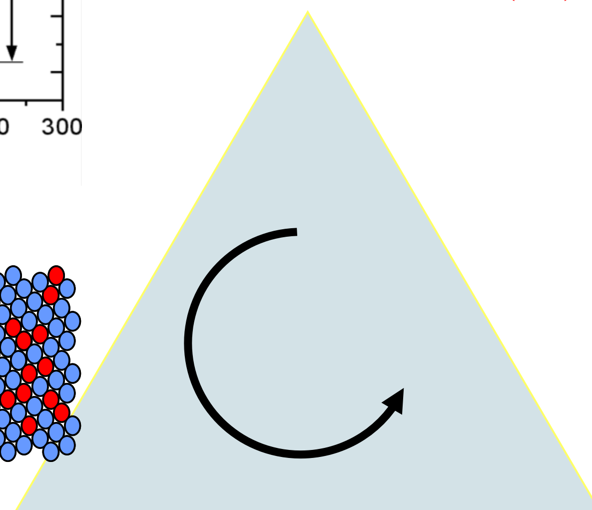

Thermal Stability

$$E_B \cong K_u V \left[1 - \frac{|H_d|}{H_0}\right]^{\frac{3}{2}}$$

K_uV = 40-80 k_BT

Writability

$$H_0 = \alpha \frac{2K_u}{M_s} - N_{eff} M_s$$

H_0 < Head Field

D. Weller and A. Moser, “Thermal Stability Limits in Magnetic Recording” IEEE Trans. Mag. 35 4423 (1999) IBM

Smallest thermally stable grain size - details

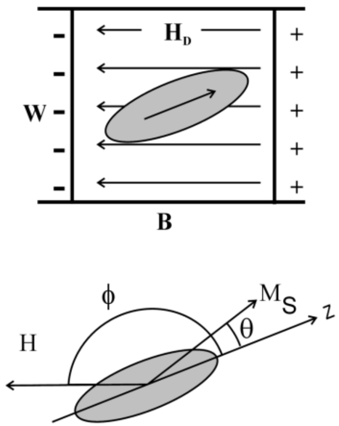

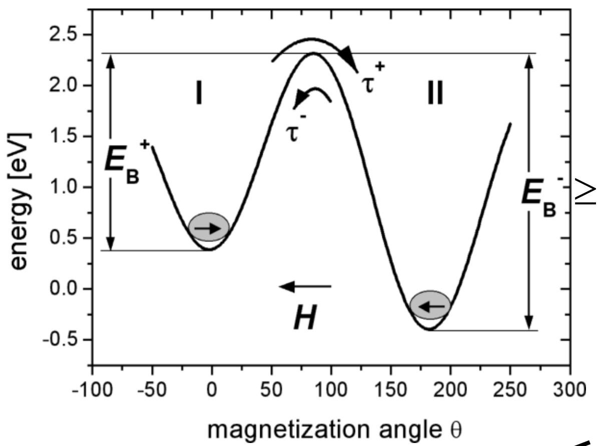

≥1.2 eV

$$\tau = f_0^{-1} e^{E_B / k_B T_S}$$

$$E_B = K_u V \left(1 - \frac{4\pi M_S}{H_K}\right)^2$$

f_0: attempt frequency $\cong \alpha\gamma H_K \cong 10^9 - 10^{12}$ Hz

$E_B/k_BT_S = \ln(f_0\tau) = r_K \sim 50$ for $\tau = 10$ years

$$D_p = \left(k \frac{2 \cdot r_K \cdot k_B T_S}{H_K M_S \left(1 - \frac{4\pi M_S}{H_K}\right)^2} \right)^n$$

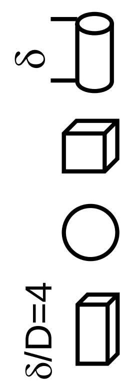

n=1/2, k=4/πδ for cylinders

n=1/3, k=1 for cubes

n=1/3, k=6/π for spheres

n=1/3, k=1/4 for prisms

D. Weller and A. Moser, “Thermal Effect Limits in Ultrahigh Density Magnetic Recording”, *IEEE Trans. Magn.*., 35, 4423 (**1999**);
D. Weller and T. McDaniel in Springer 2006 Advanced Magnetic Nanostructures, eds. D. Sellmyer and R. Skomski, chapter 11

HAMR media: high anisotropy, low Curie temp, small grains

D. Weller et al., Phys. Status Solidi A 210, 1245 (2013)

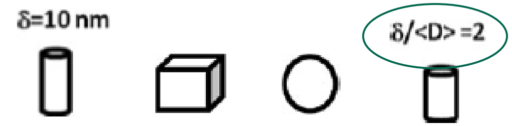

alloy system	material	K_u (10^7 erg/cm^3)	M_S (emu/cm^3)	$T = 350$ K: H_K (kOe)	$T = 350$ K: T_C (K)	D_p (a) (nm)	D_p (b) (nm)	D_p (c) (nm)	D_p (d) (nm)
Co-alloys	$CoCr_8Pt_{22}$	0.7	500	28.0	1000[a]	7.3	7.5	8.7	6.4
	Co_3Pt	2	1100	36.4	1200	4.3	5.3	6.1	4.5
PMR	$CoPt_3$	0.5	300	33.3	600	8.6	8.3	9.7	7.2
CoX/Pt(Pd) multilayers	Co_3/Pt_{10}	1.2	450	53.3	~700[b]	5.5	6.2	7.2	5.4
	Co_3/Pd_{10}	0.6	360	33.3	~700[b]	7.8	7.8	9.1	6.8
ordered	FePd	1.8	1100	32.7	760	4.5	5.4	6.3	4.7
Ll_0/Ll_1	FePt	7	1140	122.8	750	2.3	3.5	4.0	3.0
phases	CoPt	4.9	800	122.5	840	2.7	3.9	4.5	3.4
HAMR	MnAl	1.7	560	60.7	650	4.7	5.5	6.4	4.8
rare-earth transition metals	$Fe_{14}Nd_2B$	4.6	1270	72.4	585	2.8	4.0	4.6	3.4
	$SmCo_5$	20	910	439.6	1000	1.4	2.4	2.8	2.1

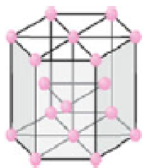

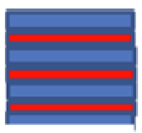

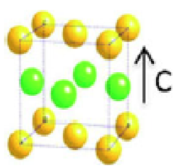

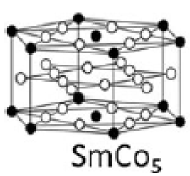

~10x higher Ku   "low" Tc   2x smaller grain dia

D_p is the average thermally stable grain diameter assuming $KV/k_BT = 60$ and $T = 350$ K, $k_B = 1.3807 \times 10^{-16}$ erg K^{-1} and volumes (a) $V = \pi/4 \times D^2 \times 10$ nm (cylinders), (b) $V = D^3$ (cubes), (c) $V = 4/3 \times \pi \times (D/2)^3$ (spheres) and (d) $V = \pi/4 \times D^2 \times \delta$ (cylinders with $\delta/D = 2$). The thickness δ is 10 nm or larger in today's media but will drop for smaller diameters going forward.

[a] T_C in today's alloy media depends on the Cr and Pt content and has increased.

[b] T_C in multilayers strongly depends on the Co thickness.

Composition and growth temperature of $Co_{1-x}Pt_x$ alloys

25 at% Pt

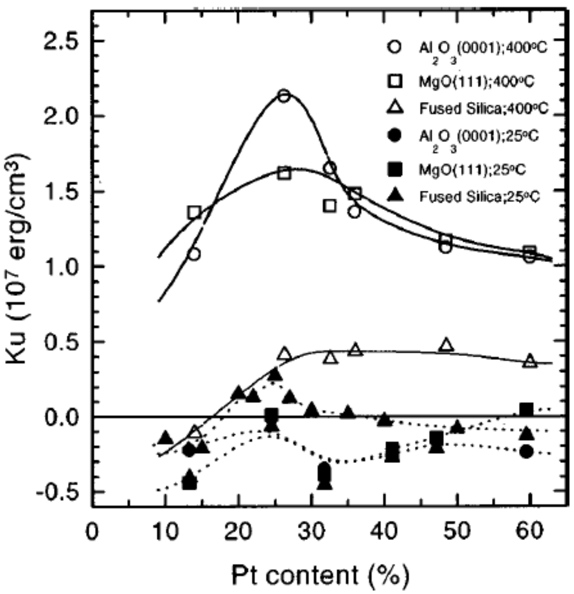

400°C

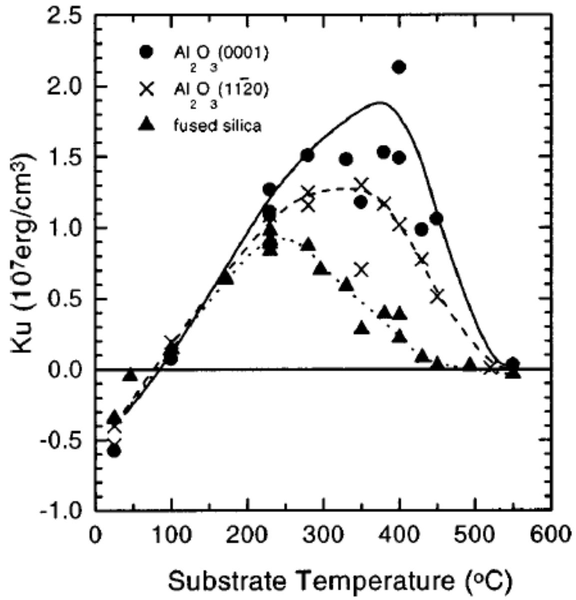

S=0.5

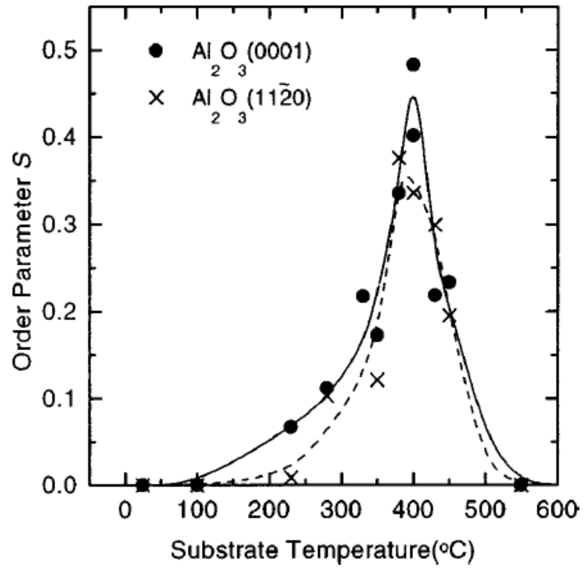

Y. Yamada, W. P. van Drent, E. N. Abarra, and T. Suzuki, "High perpendicular anisotropy and magneto-optical Activities in ordered Co_3Pt alloy films" JAP 83, 6527 (1998)

Narrowing Grain Size and Distribution

CURRENT ← CoCrPt →

FUTURE

1990 LMR

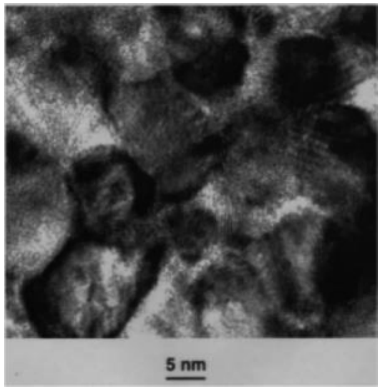

10 Gbit/in^2
product media

12 nm grains

$\sigma_{area} \cong 0.9$

J. Li, *et al.*,
J. Appl. Phys. 85, 4286 (1999)

2000 LMR

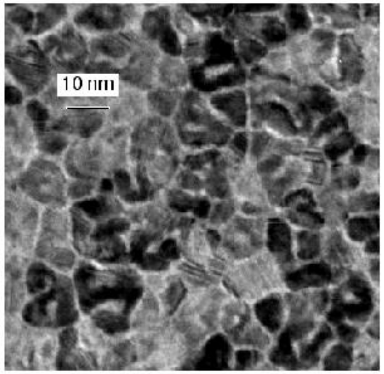

35 Gb/in^2
prototype media

8.5 nm grains

$\sigma_{area} \cong 0.6$

M. Doerner *et al.*,
IEEE Trans. Mag. 37 (2001) 1052

2008 PMR

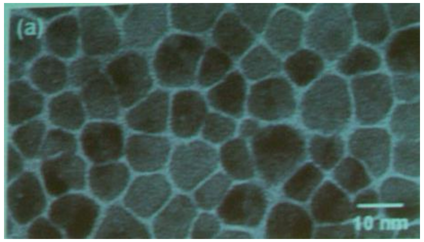

600 Gb/in^2
prototype media

8.5 nm grains

$\sigma_{area} \cong 0.36$

Tanahashi *et al.*
TMRC 2008

FePt
HAMR, SOMA

S. Sun *et al.*,
Science 287, 1989 (2000)

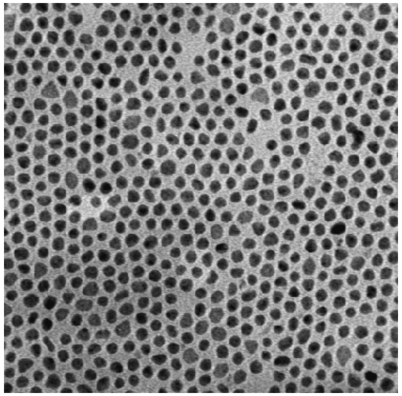

Nanoparticle arrays

4 nm particles

$\sigma_{area} \cong 0.05$

Current PMR product densities of ~ 750 Gb/in^2 are extendable to ~1-1.3 Tb/in^2
Future HAMR technology may start around 1-1.5 Tb/in^2

Key: the number of grains per bit went down from 1000 to < 10

note: $\sigma_{area} = 2x\ \sigma_{diameter}$

SOMA FePt Nanoparticles – fcc-fct phase transformation

- Annealing leads to formation of ordered, high-K_U ferromagnetic phase
- It also leads to particle agglomeration & disorder in the array

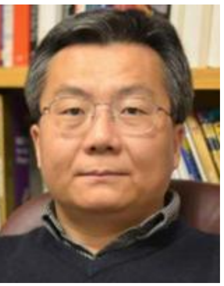

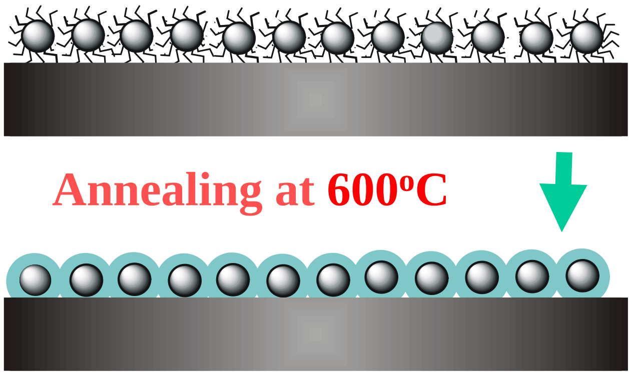

chemically disordered
fcc structure
superparamagnetic

chemically ordered
fct structure
ferromagnetic

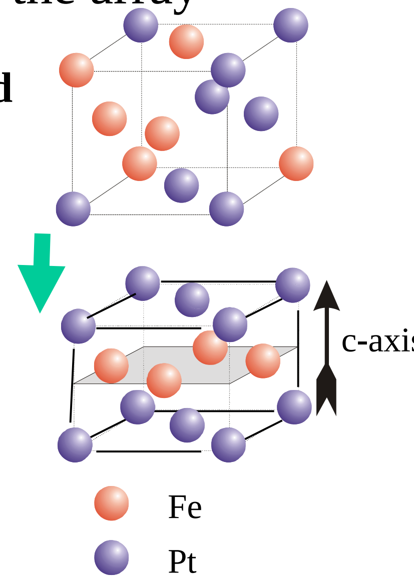

A1

a/c=1

$L1_0$

a/c~0.96

oleic acid and oleyl amine stabilizers

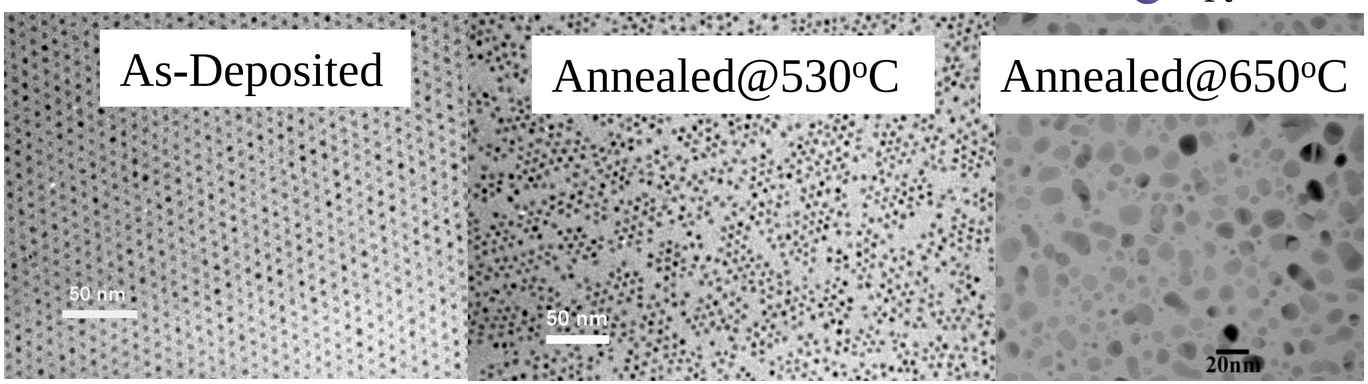

S. Sun, **C.B. Murray**, D. Weller, L. Folks, A. Moser, "Monodisperse FePt Nanoparticles", Science 287, 1989 (2000)
TJ Klemmer, C Liu, N Shukla, XW Wu, D Weller, "Combined reactions & $L1_0$ ordering", JMMM 266, 79 (2003)

HAMR

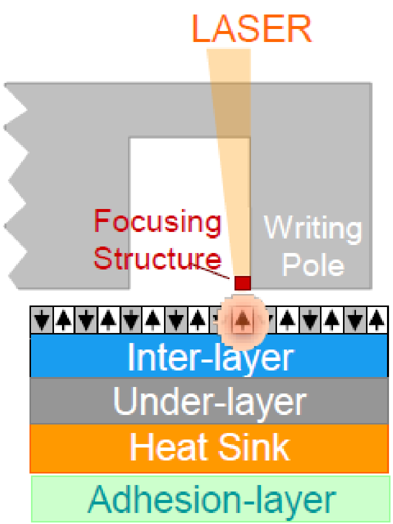

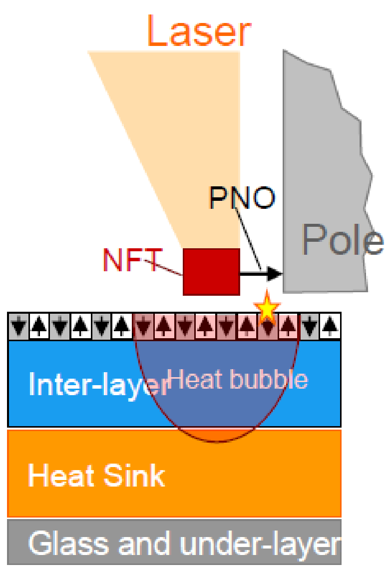

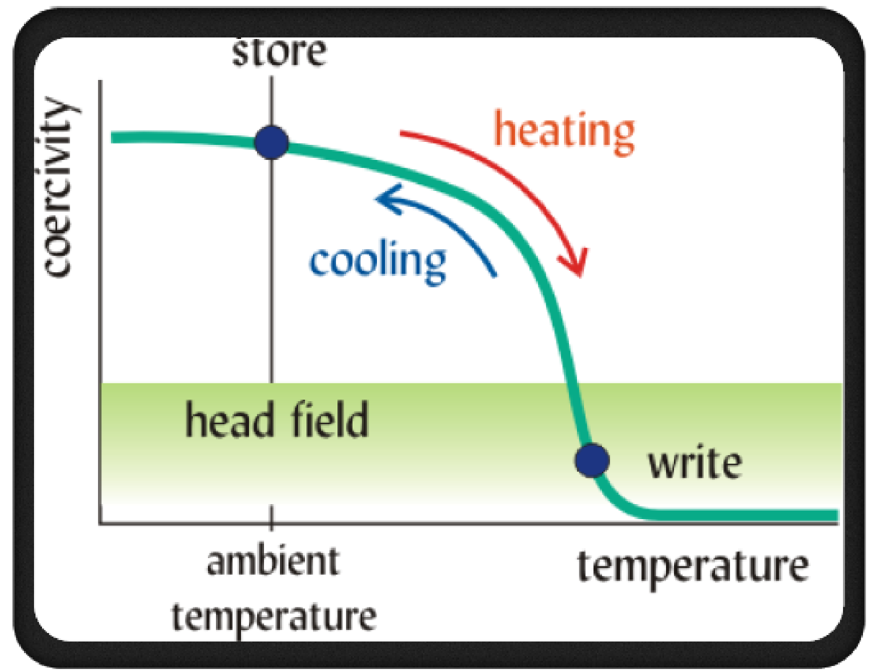

Next major technology for AD extendibility with minimal system impacts.

To record on this type of media we must first heat the media until it becomes writeable with conventional recording fields

Sputtered HAMR Media Stack

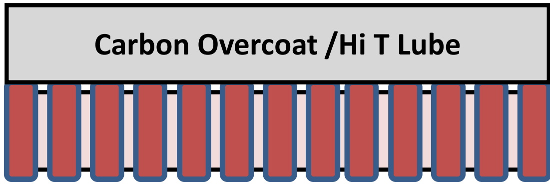

FePt + segregant X

Segregants promote grain isolation and define grain shape

Carbon, SiO_2, SiN_x, B_2O_3

other nitrides, oxides, carbides

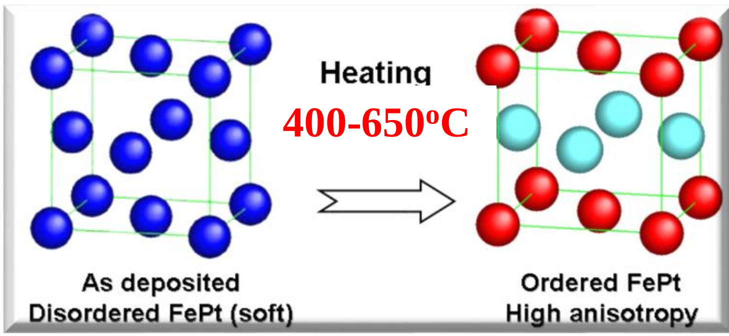

Heating

A1 – $L1_0$ chemical ordering transition

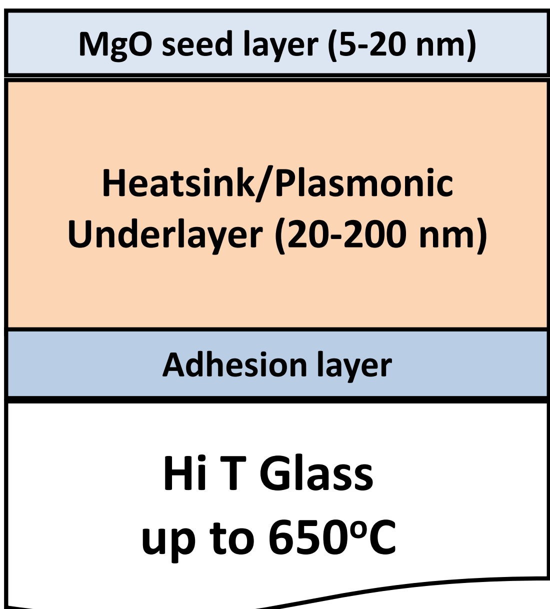

Seed layer for $L1_0$ order for FePt

MgO: FCC rocksalt, a = 0.421nm

<001> orientation, 9% mismatch

Others: **CrRu, CrMo, TiN, TiC, Cr, Ag, Pt**

Heat Sink / Plasmonic Underlayer: smooth

Examples: **Ag, Al, Cu, Cr, Au, NiAl, NiTa**

Adhesion layer

Example: **NiTa**

“Early” FePt HAMR media microstructure – spherical grains

Granular FePtAg-C media grown at ~550ºC 2011

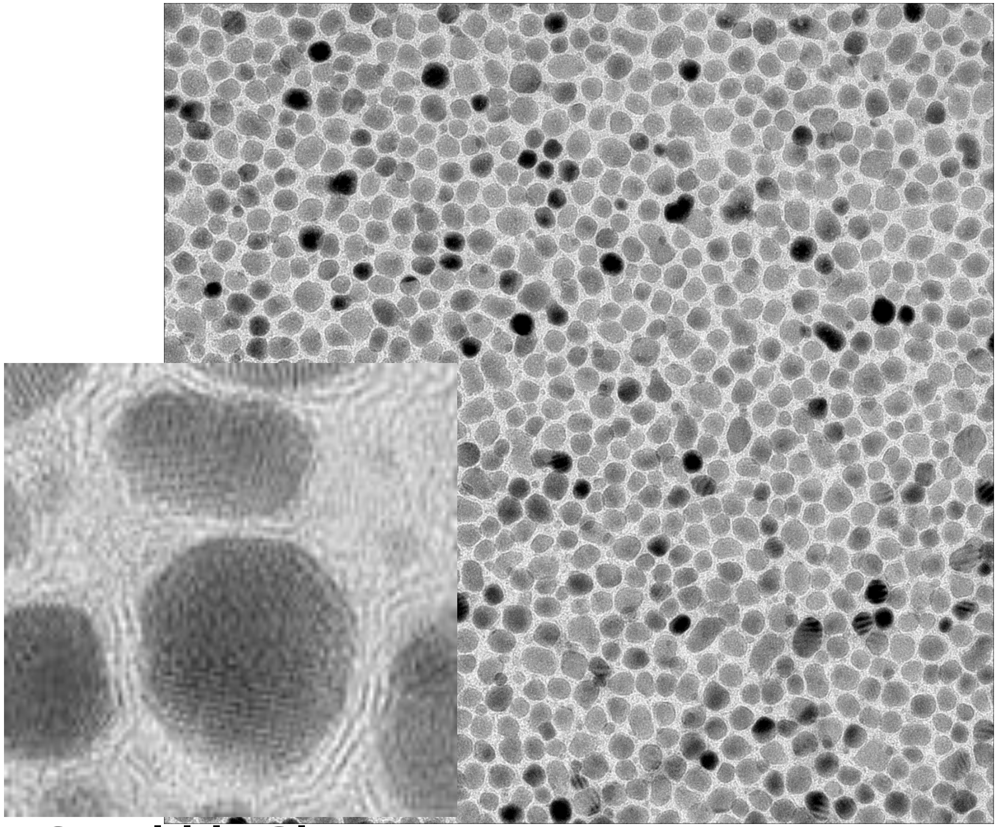

Graphitic Sheets

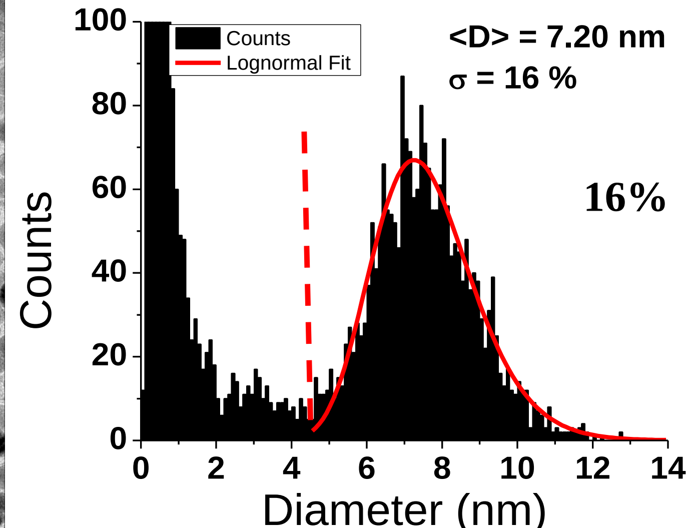

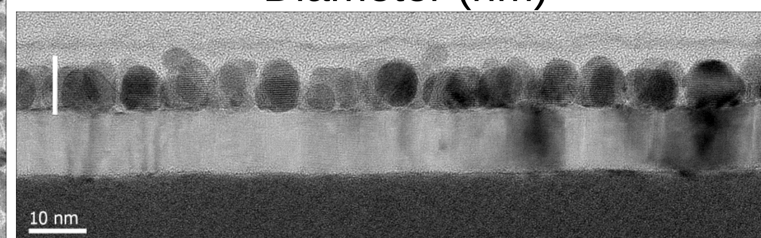

- Used a new Lean 200 sputter tool w/ 20 chambers
- Low thickness $\delta \sim 7$ nm and relatively high roughness
- Average grain size <D>~7.2 nm, grain pitch <P>~9 nm
- grain aspect ratio δ/D~1
- many small grains D<3 nm (thermally unstable)

 O. Mosendz, et al., J.Appl. Phys. 111, 07B729 (2012)

Importance of Columnar Grains

Spheres *VS.* **Columns**

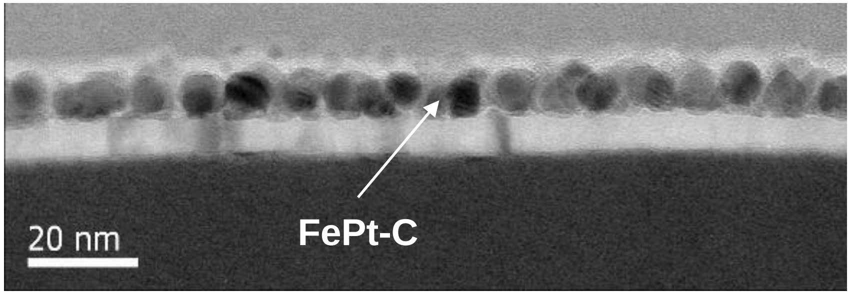

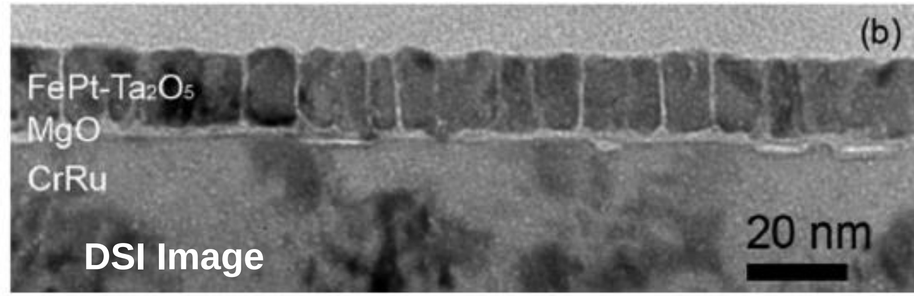

Graphitic Sheets

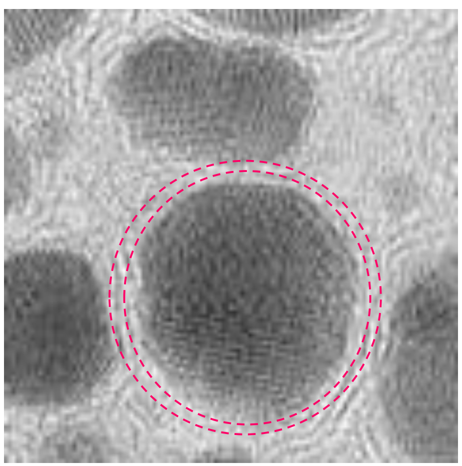

<u>Advantages of columnar grain growth</u>:

- **Decouple grain diameter from grain thickness.**
- **Thicker media will increase readback signal.**
- **Smoother surfaces and better flyability.**
- **Get laterally smaller, thermally-stable grains.**
- **Narrow distribution in optical absorption and consistent vertical heat flow from grain to grain.**
- **Enable functional layered structures.**

DSI: Data Storage Institute, Singapore

K. Hono - Nat'l Institute of Materials Science Japan (NIMS)

FePt-C as template + $FePt$-TiO_2 for columnar growth

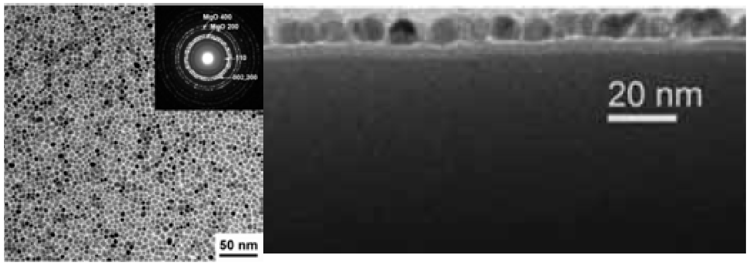

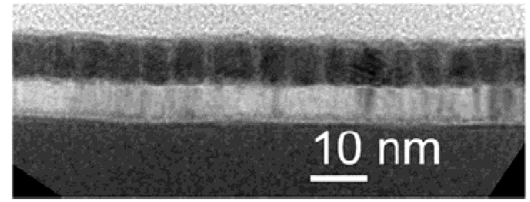

K. Hono
2013 ASTC
presentation

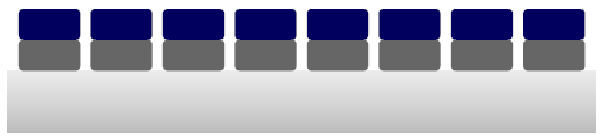

dual mag layers

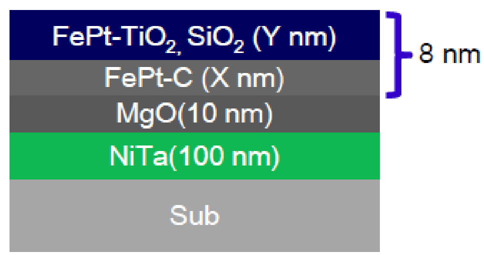

C segregant (40 vol%)	SiO_2 or TiO_2 segregants (50 vol%)
1. Good particle separation	1. Poor particle separation
2. High degree of $L1_0$ ordering	2. Poor degree of $L1_0$ ordering
3. Spherical type grains	3. Cylindrical type grains
4. Rough surface	4. Excellent surface smoothness

Currently working on C and Y_2O_3 or Cr_2O_3 segregants to combine these 2 effects

FePt dual layer media with more cylindrical grains 2012

Granular FePtX-C/Y media grown at ~620°C

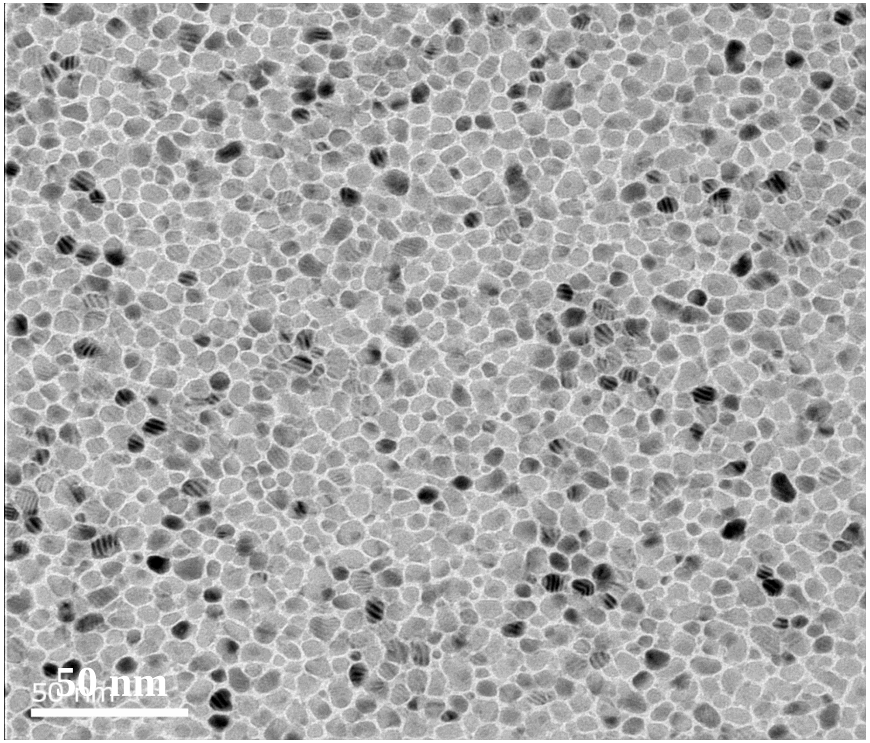

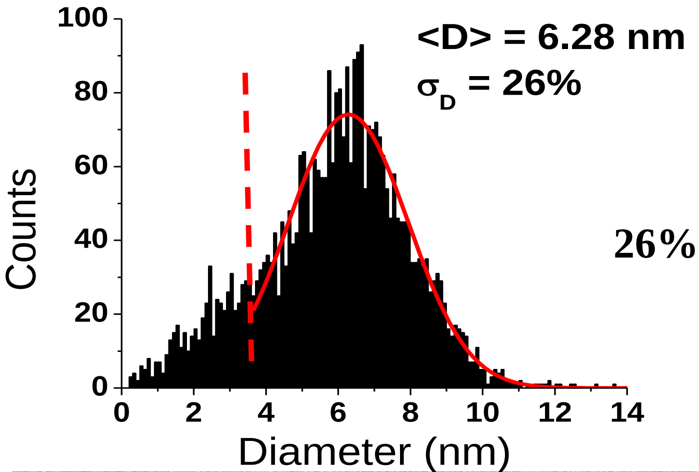

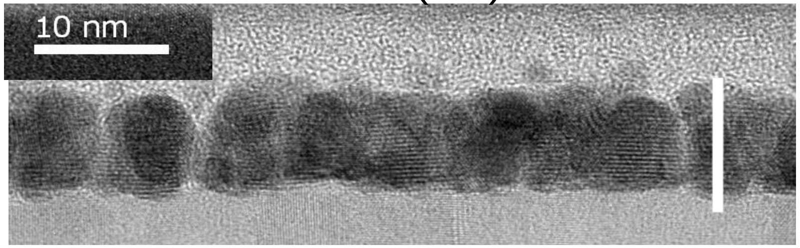

- **higher thickness δ ~ 10 nm → improved read back signal**
- **average grain size <D>~6.3 nm, grain pitch~ <P>~7.3 nm**
- **grain aspect ratio δ/D~1.6**
- **less grains with D < 3.5 nm**
- **smoother surface**
- **BUT: "worse" grain size distribution**

D. Weller et al., Phys. Status Solidi **A 210**, 1245 (2013)

FePt triple layers w/ less smaller grains 2013

Granular FePtX-Y media grown at ~640°C

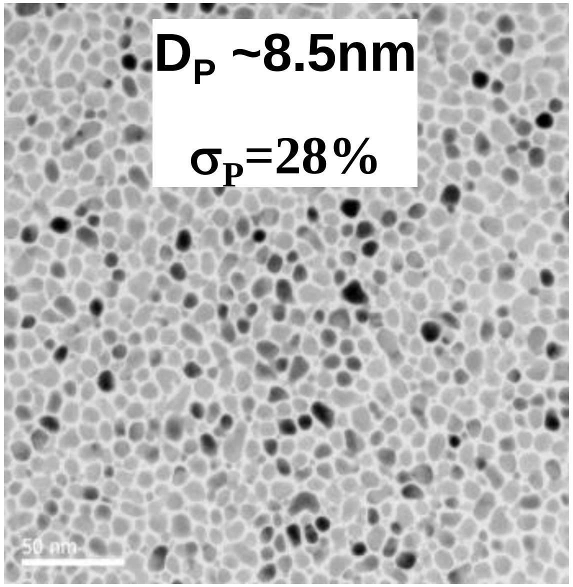

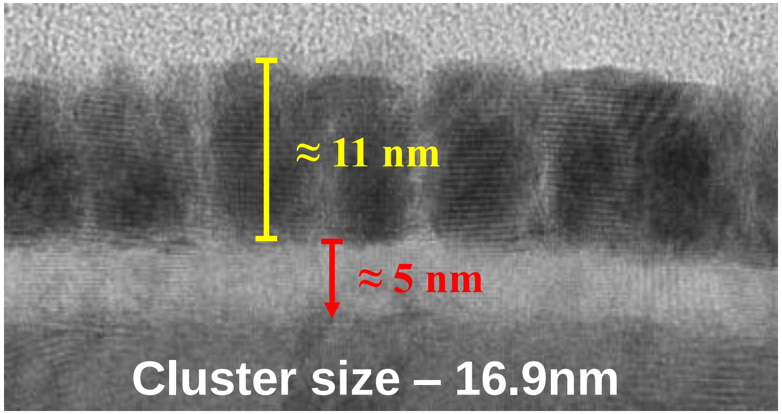

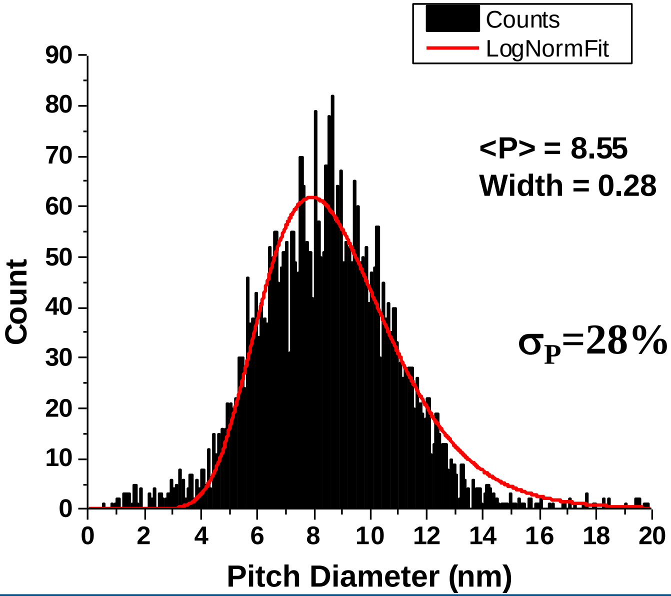

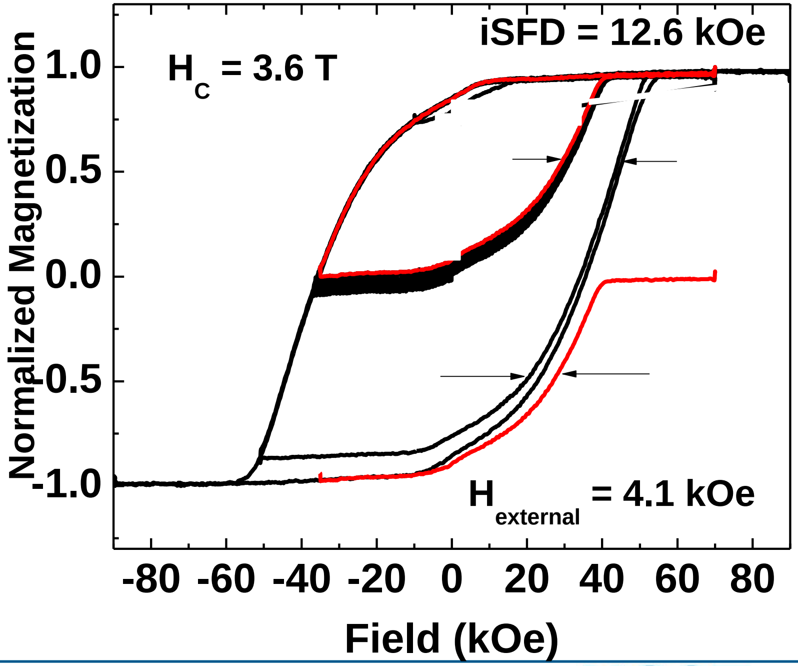

Improved grain size distribution 2014

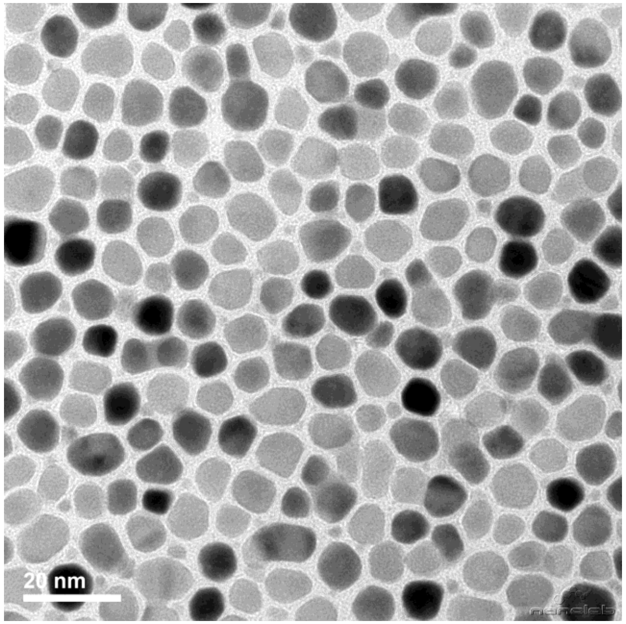

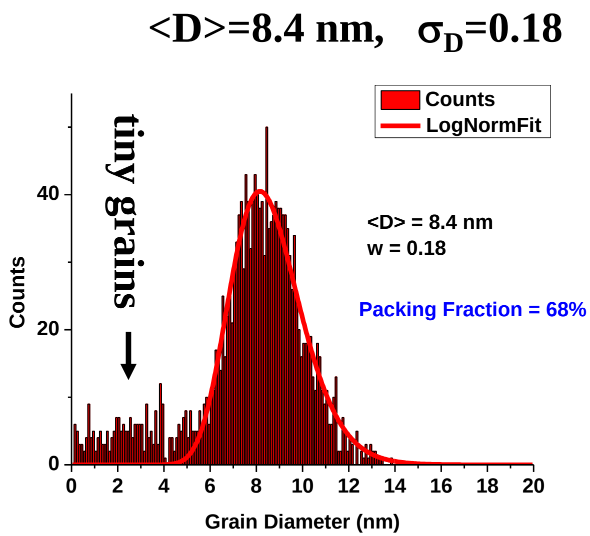

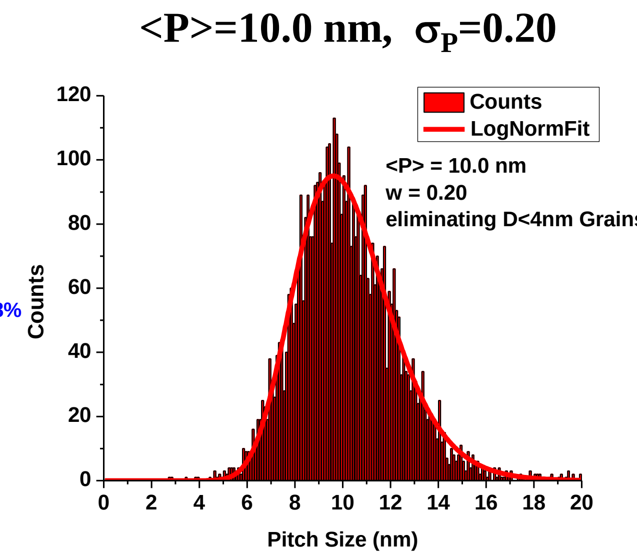

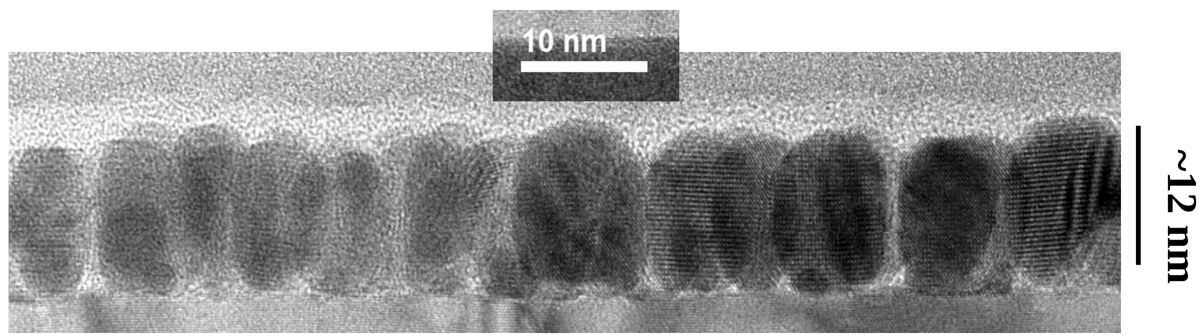

Packing fraction = 68%
$\langle D\rangle=8.4$ nm, $\sigma_D=0.18$
$\langle P\rangle=10.0$ nm, $\sigma_P=0.20$
$\delta/D\sim1.5$

- **reduced amount of tiny grains**
- **significantly improved size distribution**

HAMR media microstructure evolution

Thickness d=7 nm | Thickness d=10 nm | Thickness d=12 nm

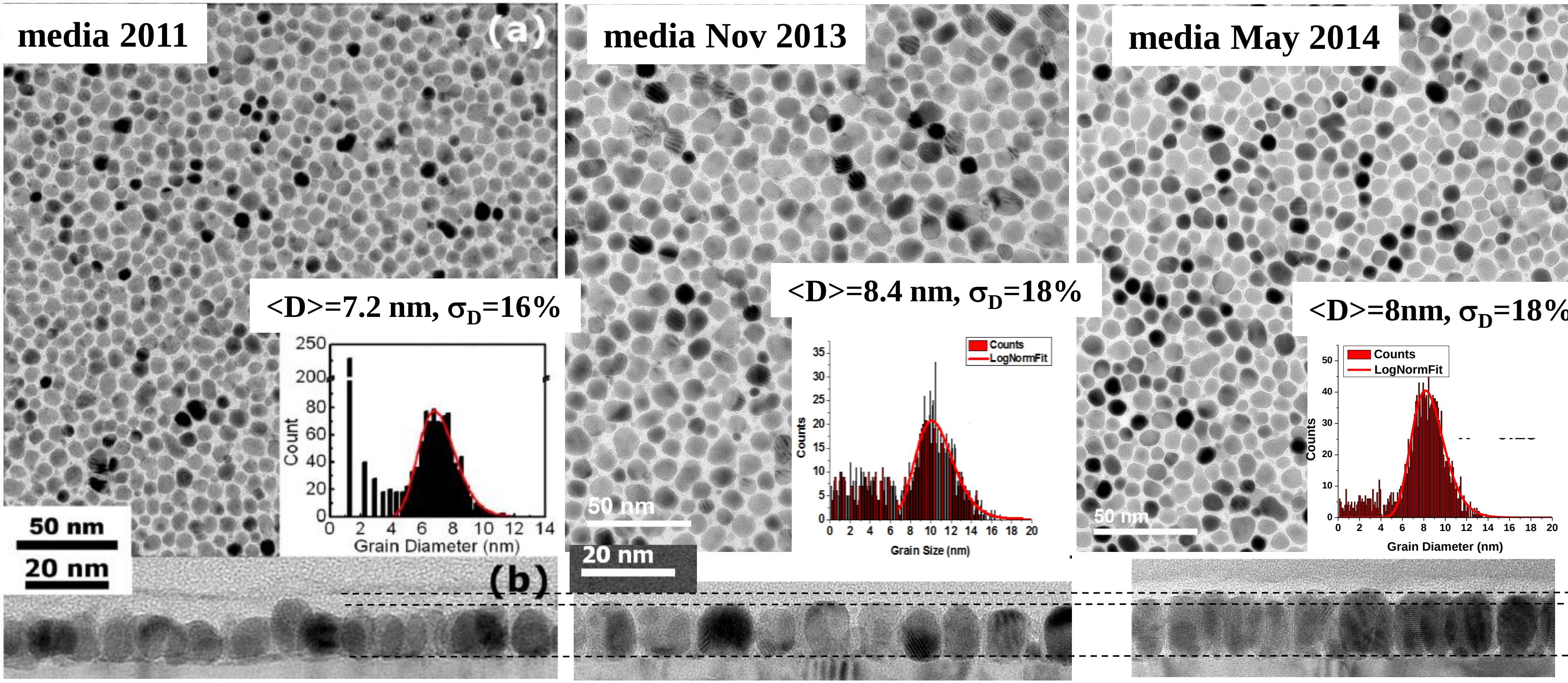

- small grains
- tight size distribution
- spherical grains
- low signal
- rough media

- larger grains
- tight size distribution
- more columnar grains
- increased signal
- reduced roughness

- smaller grains
- tight size distribution
- columnar grains
- further increased signal
- smoother surface

Minor Loop Analysis: Switching Field Distribution (300K) 2011

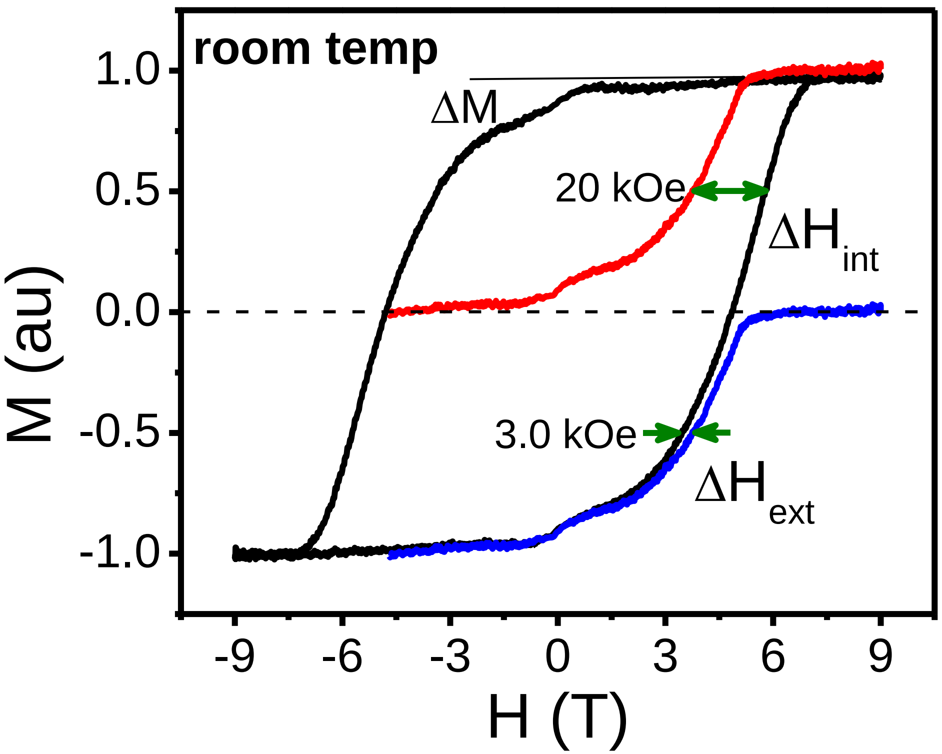

What is iSFD at the recording temperature, near Tc ?

Small *eSFD* → small cluster size (14nm) → low exchange and magnetostatic interactions

Large *iSFD*: $\sigma_{\text{int}}^{2} = \sigma_{vol}^{2} + \sigma_{\text{axis}}^{2} + \sigma_{Hk}^{2}$

σ_{int} = 15 kOe (VSM)

Grain volume distribution: **σ_{vol} = 3.7kOe**

- from TEM grain size analysis

Grain texture distribution: σ_{axis} = 6.6kOe

- from rocking curve width, XRD

Anisotropy distribution: **σ_{HK}=12.9kOe**

- from VSM, may arise from variations in $L1_0$ order, lattice strain & defects

Micromagnetic model needed to go beyond these estimates

S. Pisana et al., Effects of grain microstructure on magnetic properties in FePtAg-C JAP 113, 043910 (2013)

Magnetic properties of "early" FePt-C samples 2011

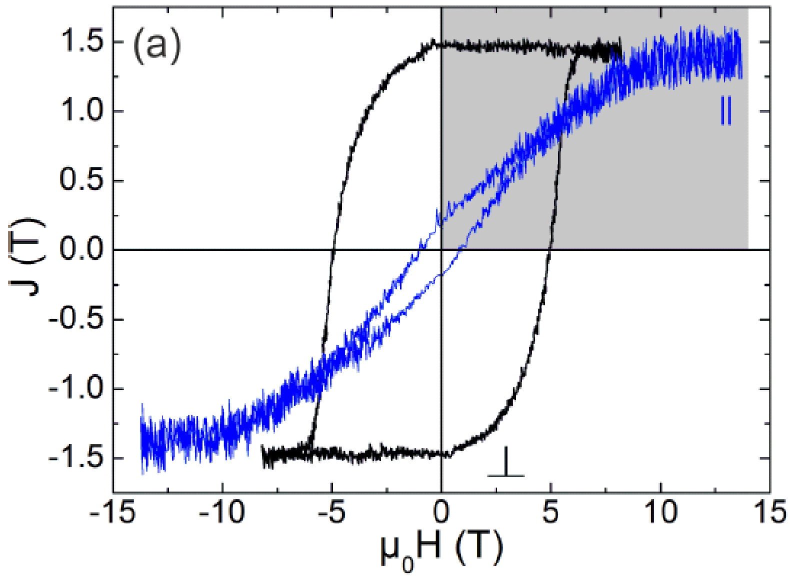

S. Wicht, V. Neu, L. Schultz, B. Rellinghaus, D. Weller, O. Mosendz,, G. Parker, and S.Pisana, **"Atomic resolution structure–property relation in highly anisotropic granular FePt-C films with near-Stoner-Wohlfarth behaviour"** J. Appl. Phys. **114**, 063906 (2013)

IFW Dresden

H_C ~ 5T H_K ~10T M_S ~ 1040 emu/cm^3 at 290K
K_U ~ 5.2 x 10^7 erg/cm^3 <D>=nm grain diameter

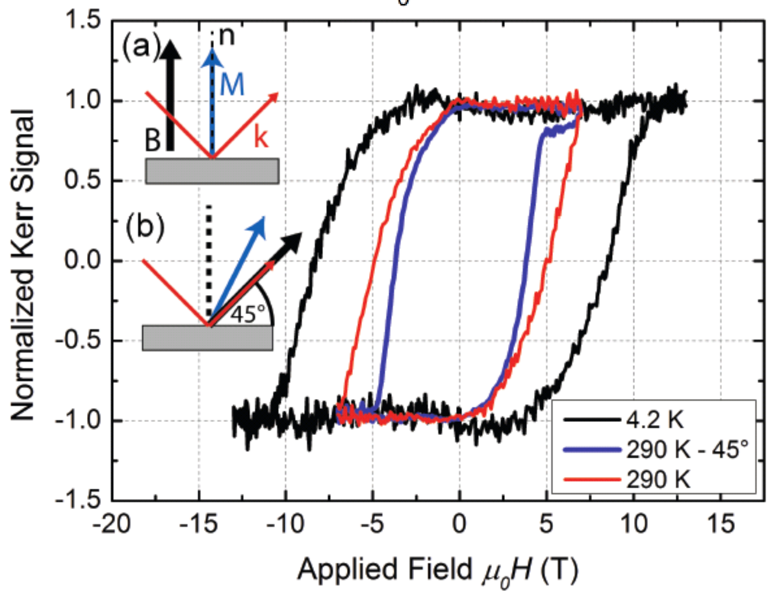

J. Becker, O. Mosendz, D. Weller, A. Kirilyuk, J.C. Maan, P.C.MM. Christianon, Th. Rasing and A. Kimel, **"Laser Induced Spin Precession in Highly Anisotropic Granular L1$_0$ FePt"**, Appl. Phys. Lett. **104**, 069416 (2014)

Radboud University, Nijmegen

H_C~5T H_K ~10T M_S ~ 950 emu/cm^3 at 290K
K_U ~ 4.8 x 10^7 erg/cm^3
H_C = 8.2T at 4.2K
α ~ 0.1 damping parameter in FMR

XRD and MOKE hysteresis of improved media 2013

(001)/(002) XRD ratio 1.9 – 2 → chemical ordering S~0.90

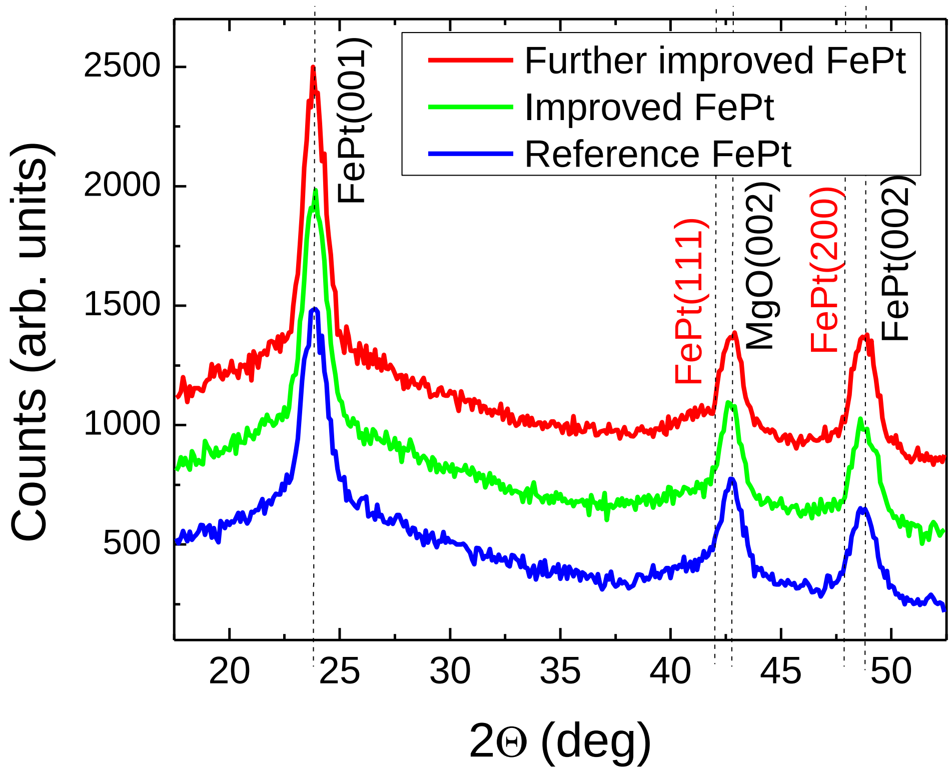

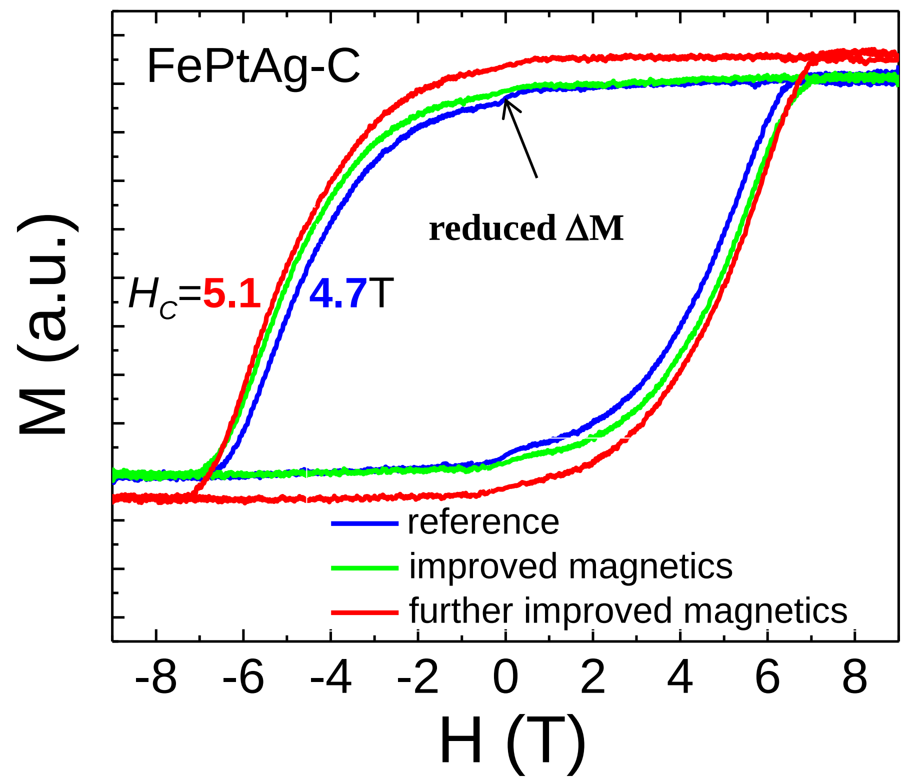

Modified deposition parameters result in suppression of very small grains and reduced noise in recorded media

D. Weller et al., Phys. Status Solidi A 210, 1245 (2013)

Quantifying amount of in-plane easy axis grains with XRD and VSM

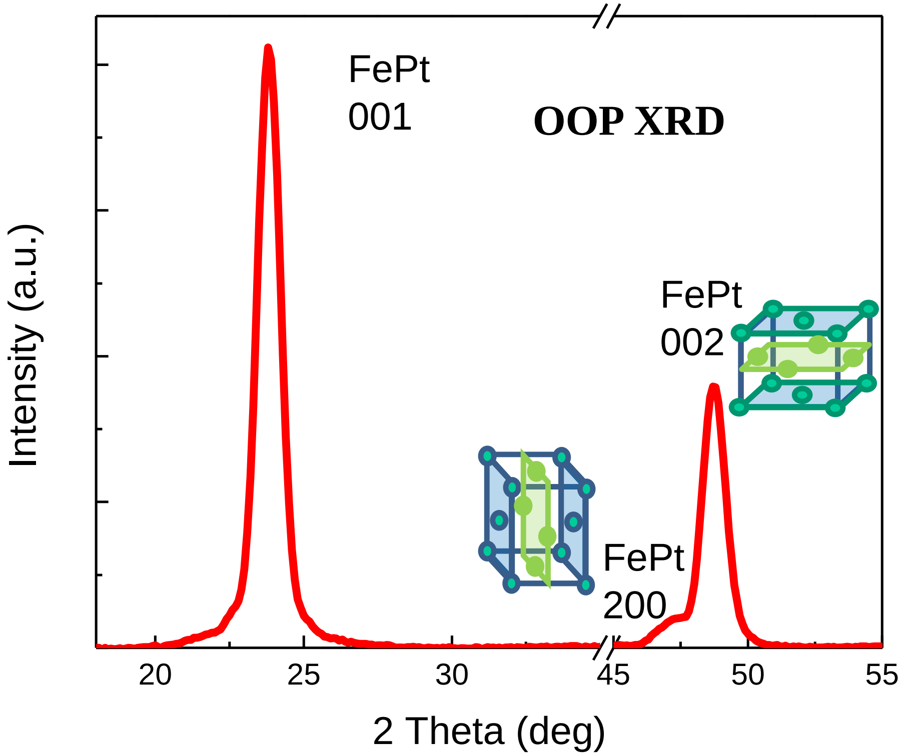

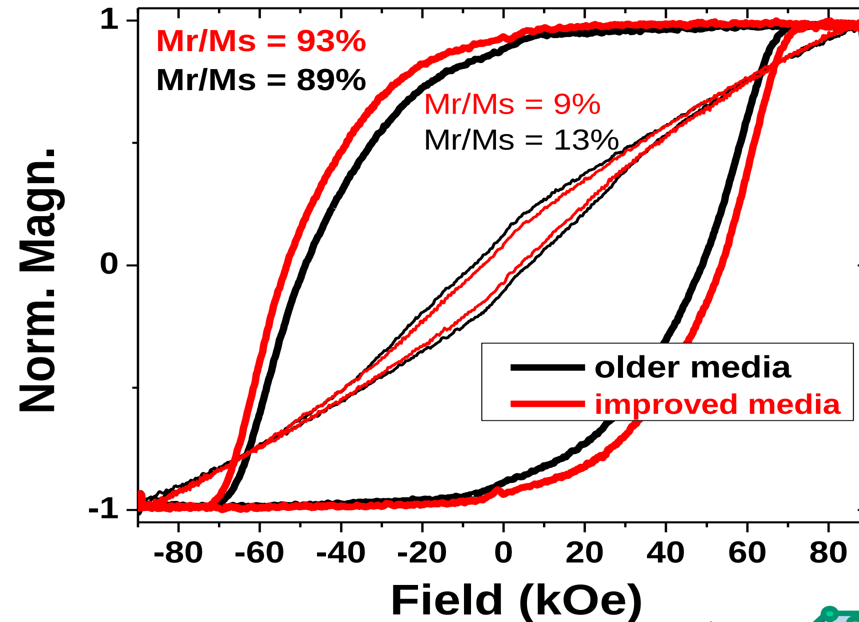

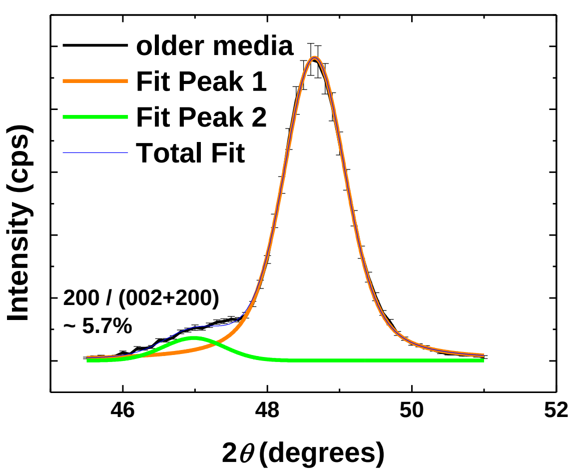

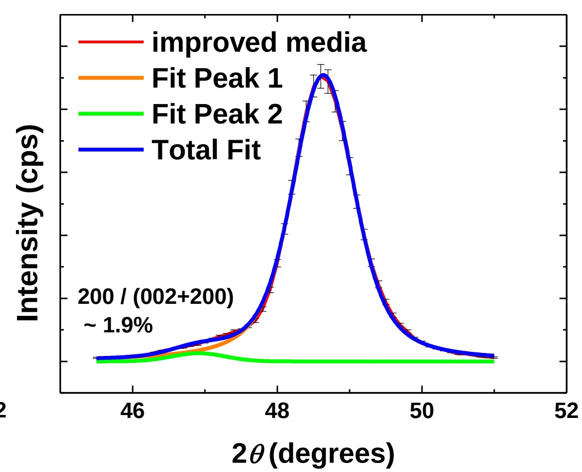

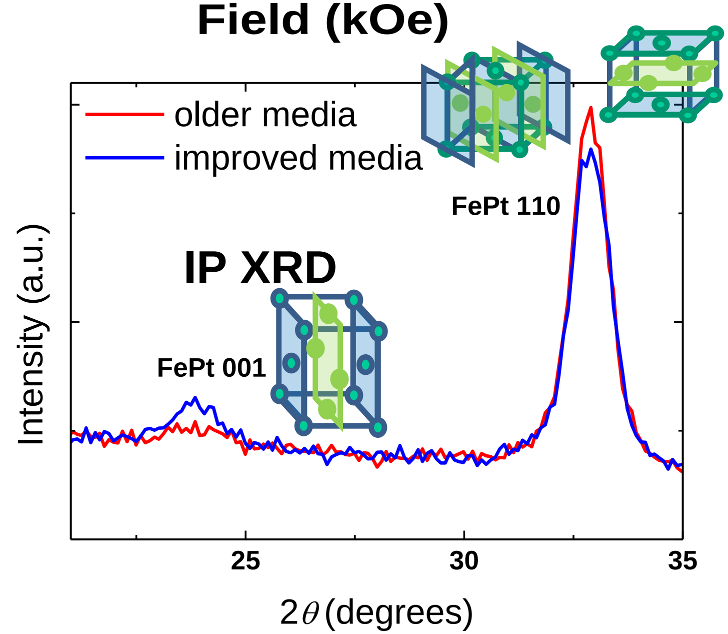

Chemical ordering S and Curie temperature T_C vs grain size

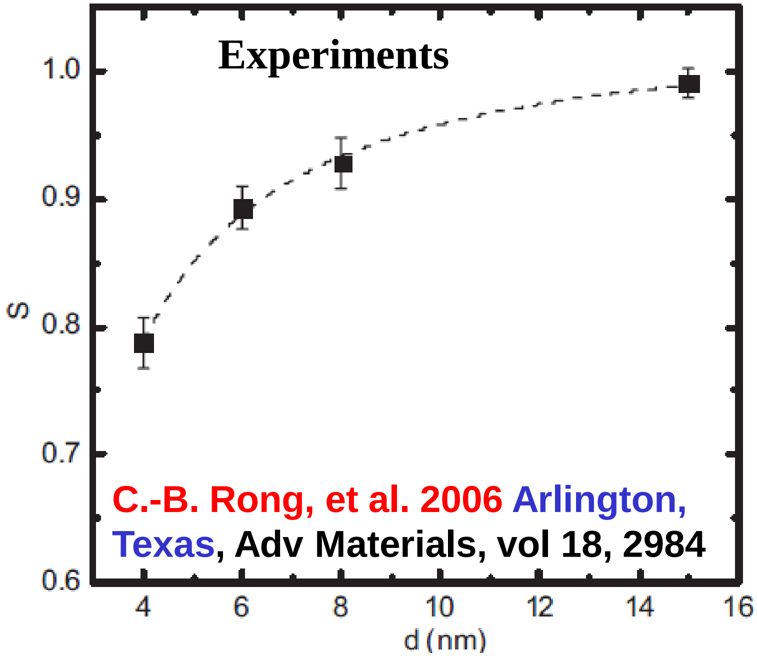

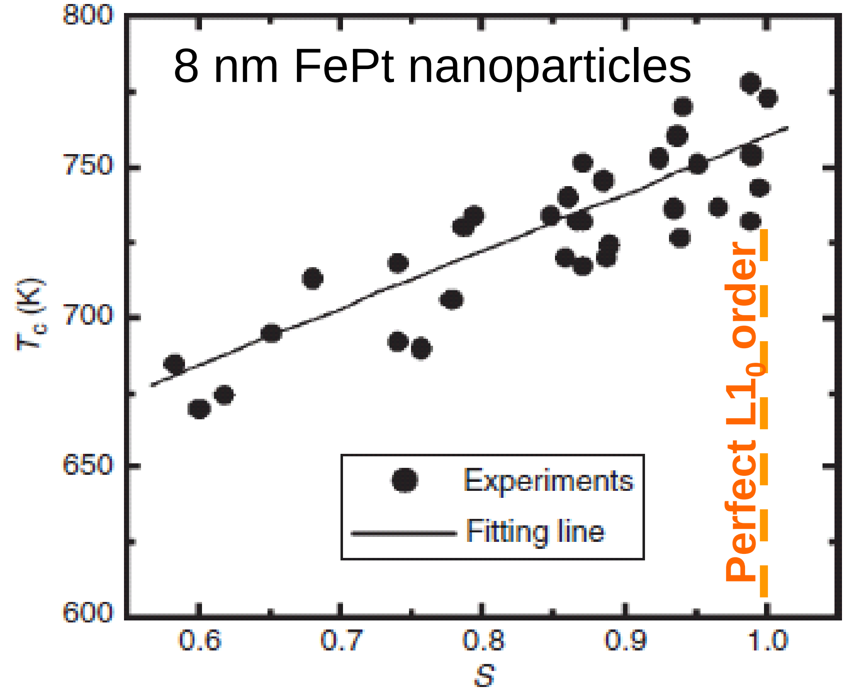

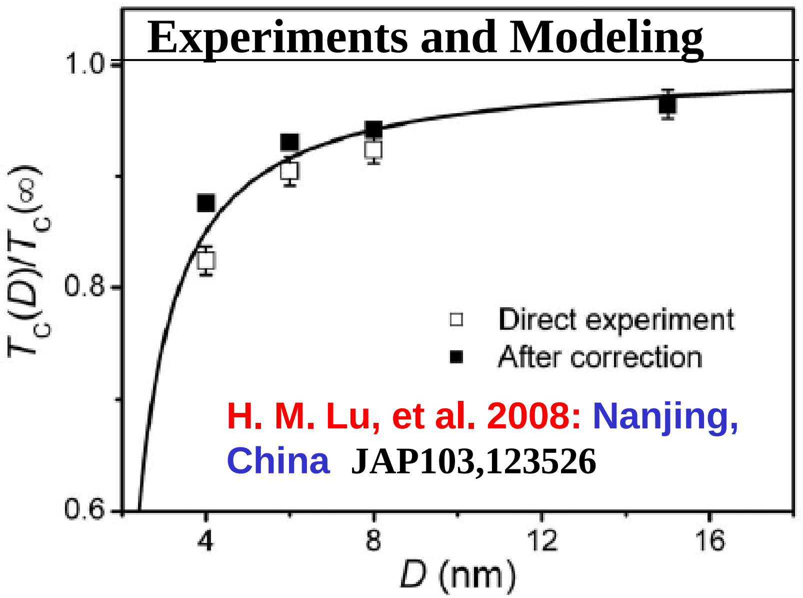

Recent Modeling by Seagate and HGST

O. Hovorka, ….., G. Ju, R. W. Chantrell, 2012: "The Curie temperature distribution of FePt granular magnetic recording media", APL 101, 052406 York U. – Seagate

A. Lyberatos, D. Weller, G. Parker, 2012: "Size dependence of the T_C of $L1_0$-FePt nanoparticles" JAP 112,113915 Crete U. – HGST

see: D. Weller et al, "The HAMR Media Technology Roadmap to an Areal Density of 4 Tb/in^2" IEEE Trans Mag 50, 3100108 (2014)

Effect of grain size and aspect ratio on T_C - Modeling

Modeling

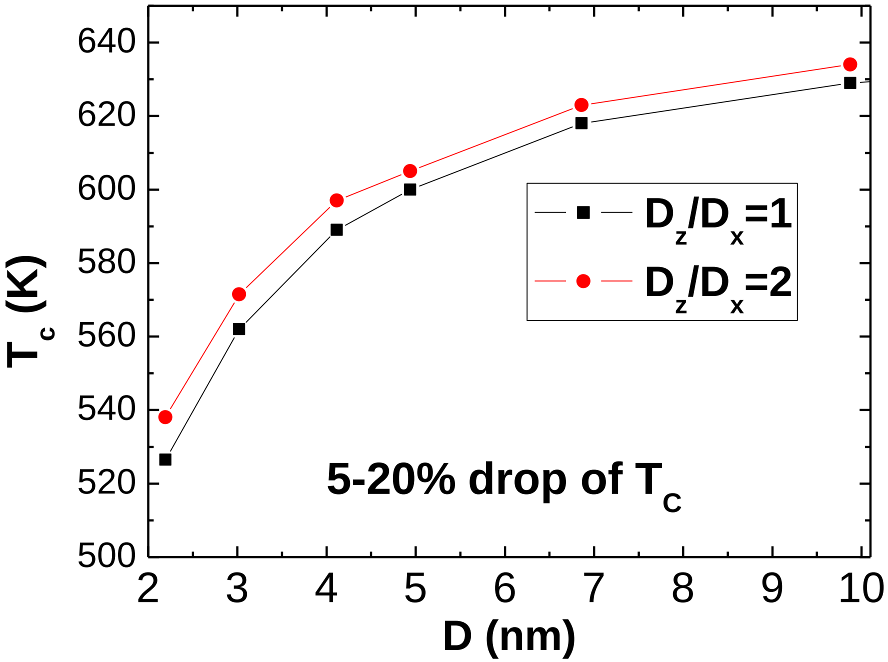

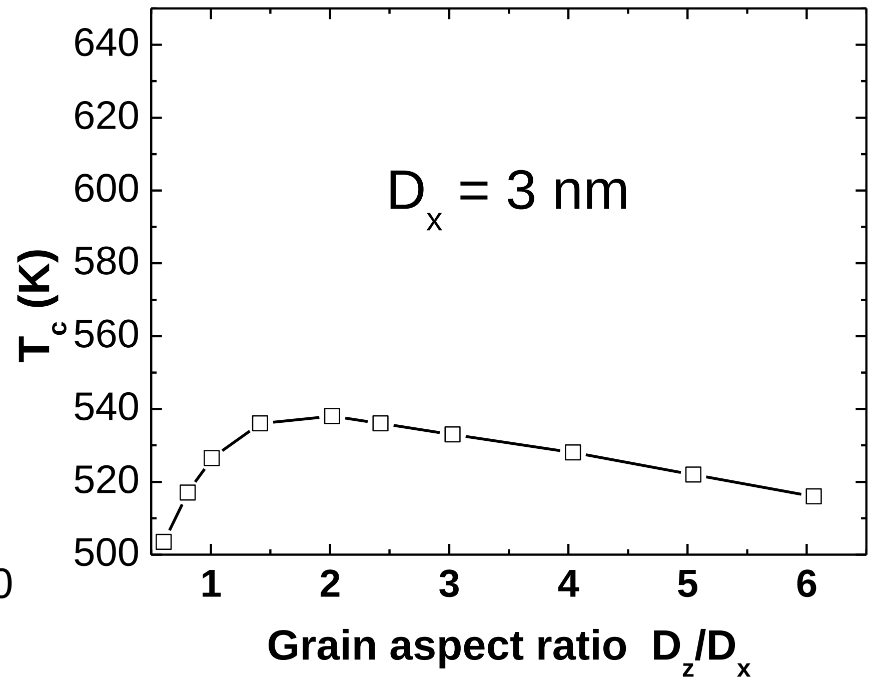

Finite size scaling theory $$T_c(D) = T_c(\infty)\left(1 - x_o D^{-1/\nu}\right)$$ **ν~0.7+/–.09**

- **T_C smaller than 750 K due to exchange truncation/abandonment in single particle modeling**
- **Cylindrical grains with an aspect ratio of ~2 reduce x_0 by ~20%, i.e. "minimize" the grain size induced reduction of T_C**
- **ν=0.7+/–0.09 is compatible with 3D Ising/Heisenberg models**
- **T_c determined from peak susceptibility χ(T) using Monte Carlo method**

A. Lyberatos, D. Weller, G. Parker, "Finite size effects in *$L1_0$*-FePt nanoparticles" J. Appl. Phys. 114, 233904 (2013)

σ_{TC} vs grain diameter D_x

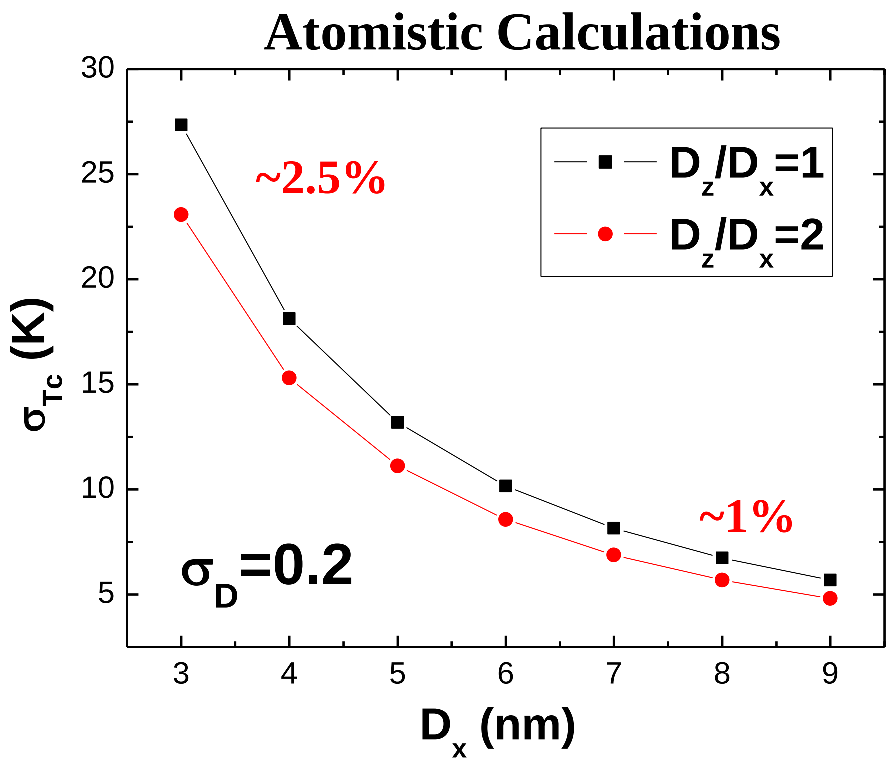

- Variations in T_c arise from the dispersion in grain size and chemical order.
- Recording performance is highly sensitive to T_c and H_K distributions.
- **Reducing D increases σ_{Tc}/T_C from ~1% (D=8nm) to ~2.5% (D=4nm).**

A. Lyberatos, et al, “Size dependence of T_C of $L1_0$-FePt nanoparticles” J. Appl. Phys.. **112**, 113915 **(2012)**

A. Lyberatos, et al, “Memory erasure and write field requirements in HAMR using $L1_0$-FePt nanoparticles” **(2014)**

HAMR Media Design Challenges

Structure-Property Relationships

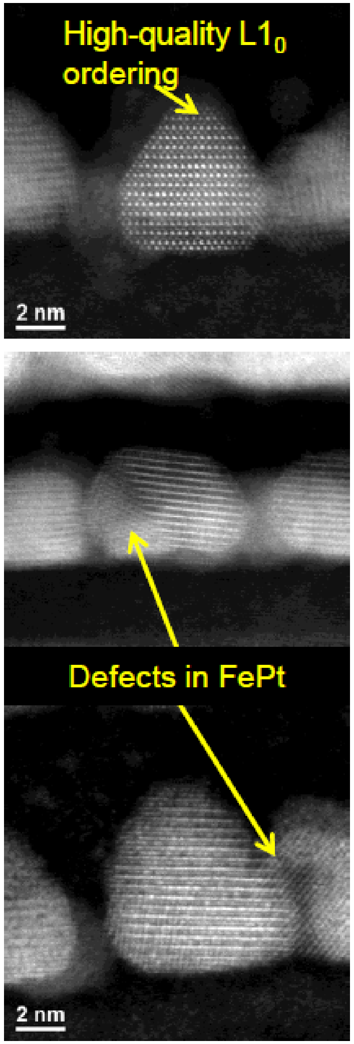

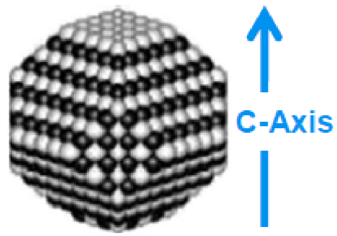

Ordered FePt

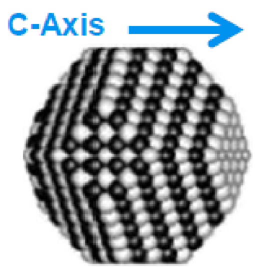

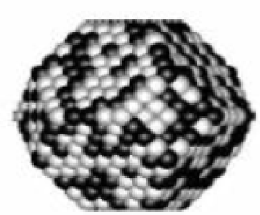

Disordered FePt

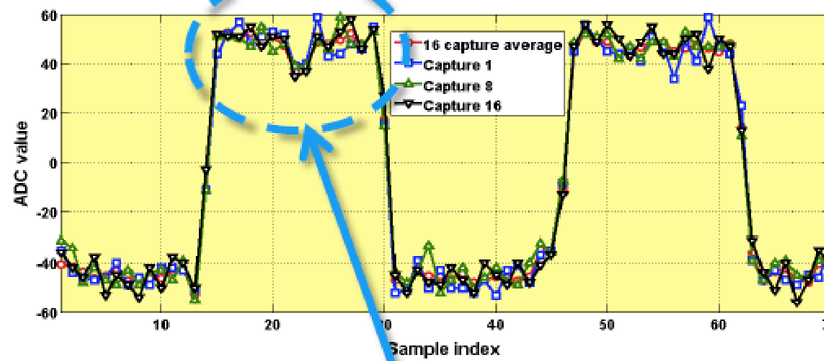

- DC Noise is still high in HAMR media
- Origin is likely caused by defected media grains
- Need to quantify problem…

Aug 12, 2014

Ramamurthy Acharya

Western Digital, 1710 Automation Parkway, San Jose, CA 95131

Contribution:

A. Ajan, A. Chernyshov, C. Papusoi, M. Chaplin, M. Desai, E. Champion, A. Moser, M. Alex, G. Bertero, M. Almaqablah, D. Tripathy, H. Yuan, S. Pirzada, T. Seki, B. Wang, O. Krupin, and B. Valcu

Starting to count individual atoms …

atom numbers	size (nm)
201	1.77
459	2.31
1289	3.27
2075	3.85
4033	4.77
5635	5.35
9201	6.31
11907	6.87

At ~3 nm diameter particles have 25-30% atoms on surface! Properties change as a result of that!

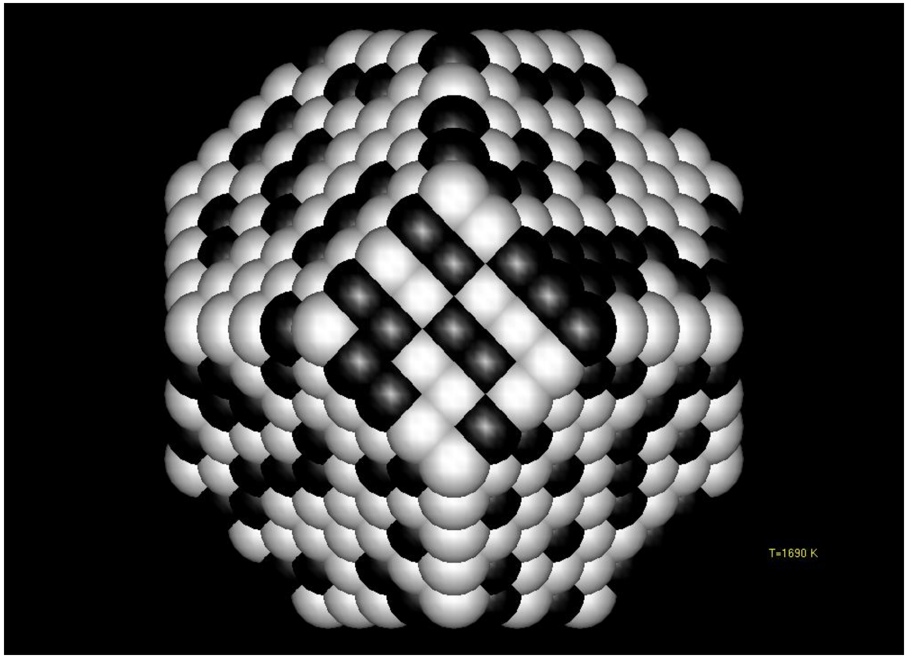

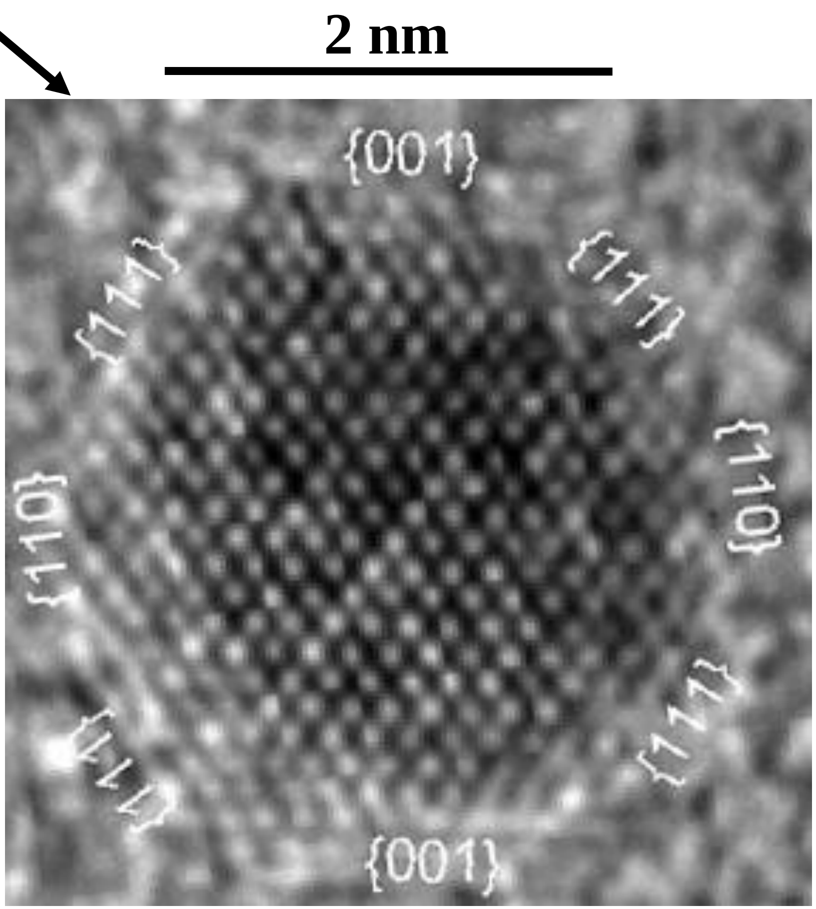

Oleg Mryasov, 2003 (Seagate)

Particle Size Effects: 3d(Fe,Co)-5d/4d(Pt/Pd) High Anisotropy Alloys

Curie Temperature Reduction

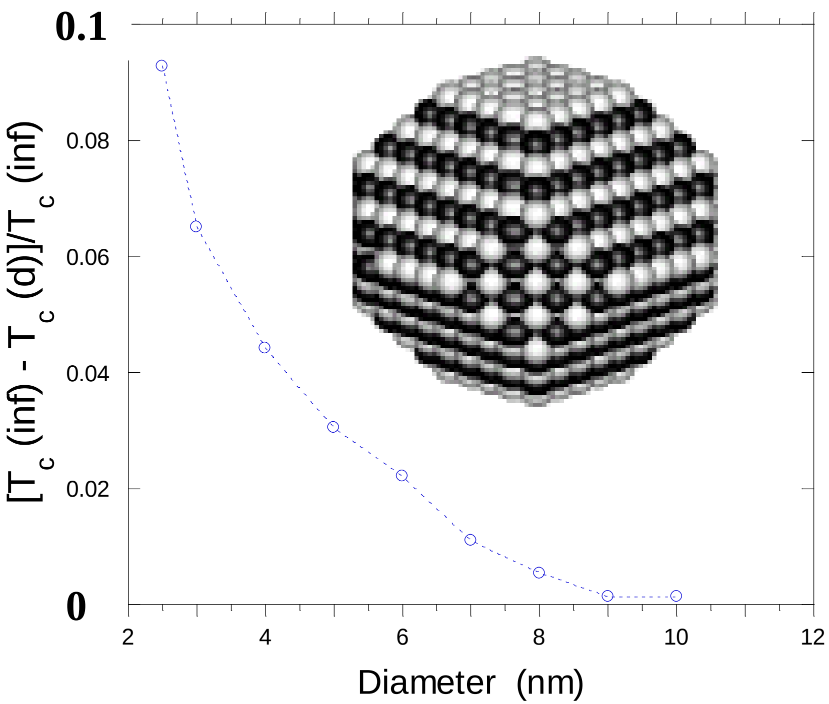

Anisotropy Energy Reduction

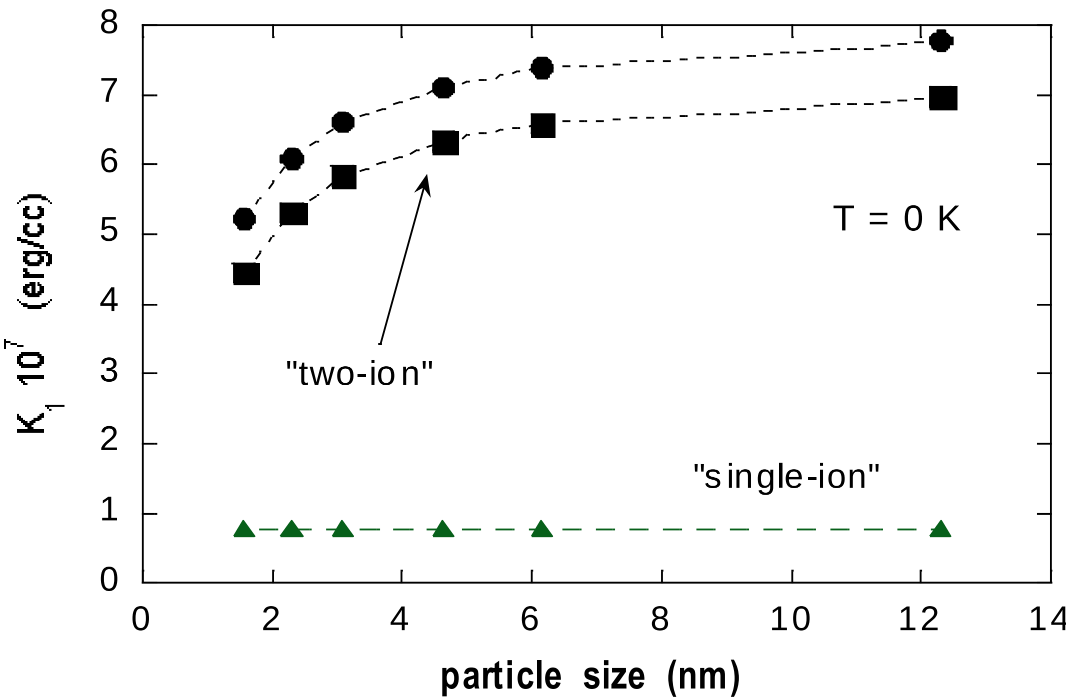

Surface to volume fraction increases to 20-40% for 3 nm FePt particles (1000 atoms)

$$d_{ij}^{(2)} = \frac{k_{Pt}^{(0)}}{[J_{\mu}^{0}]^2} \sum_{\mu} J_{i\mu}^{Fe-Pt} J_{j\mu}^{Fe-Pt}$$

Finite size effects due to interactions mediated by induced Pt magnetic moment

O. N. Mryasov - U. Nowak - K. Y. Guslienko - R. W. Chantrell, Europhy. Lett. 69, 805 (2005)

Buschow "Handbook of Magnetic Materials", Elsevier 2011, J. Lyubina, B. Rellinghaus, G. Gutfleisch, M. Albrecht

"Structure and Magnetic Properties of $L1_0$-Ordered Fe-Pt Alloys and Nanoparticles"

Table 5.2 The room temperature magnetic behaviour (para - paramagnetic; ferro - ferromagnetic; af - antiferromagnetic) and magnetic properties of the main phases in the Fe–Pt system: the Curie temperature T_c, the anisotropy constant K_1, the anisotropy field $H_A = 2K_1/\mu_0 M_s$, the saturation magnetisation M_s, the upper limit of energy density $(BH)_{max} = \mu_0 M_s^2/4$, the domain wall-width δ_w, the exchange length l_{ex} and the critical single-domain particle size D_c.

	Compound	Structure (space group)	Magnetic behaviour	T_c (K)	K_1 (MJ/m^3)	$\mu_0 H_A$ (T)	$\mu_0 M_s$ (T)	$\mu_0 M_s^2$ / 4 (kJ/m^3)	δ_w (nm)	l_{ex} (nm)	D_c (nm)	References
	α-Fe	$A2$ ($Im\bar{3}m$)	ferro	1043	0.046		2.16	928	30	1.5	7	Kneller and Hawig (1991), Skomski and Coey (1999)
Disordered	Fe_3Pt	bcc martensite[a]	para									Kussmann and von Rittberg (1950), Sumiyama et al. (1983)
	FePt	$A1$ ($Fm\bar{3}m$)	ferro	585			1.5	448	≈15			Kussmann and von Rittberg (1950), Menshikov et al. (1974)
	$FePt_3$	$A1$ ($Fm\bar{3}m$)	ferro	425			0.8	127				Bacon and Crangle (1963)
Ordered	Fe_3Pt	$L1_2$ ($Pm\bar{3}m$)	ferro	410			1.8	645	≈15			Kussmann and von Rittberg (1950), Menshikov et al. (1975), Sumiyama et al. (1978), Hai et al. (2003b)
	FePt	$L1_0$ ($P4/mmm$)	ferro	750	6.6	11.5	1.43	510	6.3	2.0	560	Kussmann and von Rittberg (1950), Ivanov et al. (1973), Vlasova et al. (2000)
	$FePt_3$	$L1_2$ ($Pm\bar{3}m$)	para (af below 160 K)									Bacon and Crangle (1963), Maat et al. (2001)

T_C =585 K

Full chemically ordered T_C =750 K

[a] fcc ($A1$) Fe_3Pt starts to transform to a bcc martensite already at room temperature (Sumiyama et al., 1983).

Strong dependence of T_C on chemical ordering A1 → $L1_O$ (ΔT_C =165K)

Kussmann, A, von Rittberg, G.Grfn., "Study of conversions in the Platinum –Iron System ", Z. Metallkd. 11, 470 (1950); A. Z. Menshikov, Yu. A. Dorofeev, V. A. Kazanzev,. S. K. Sidorov, Fiz. metal. metalloved. 38, 505 (1974).

Forming ternary alloys to improve ordering

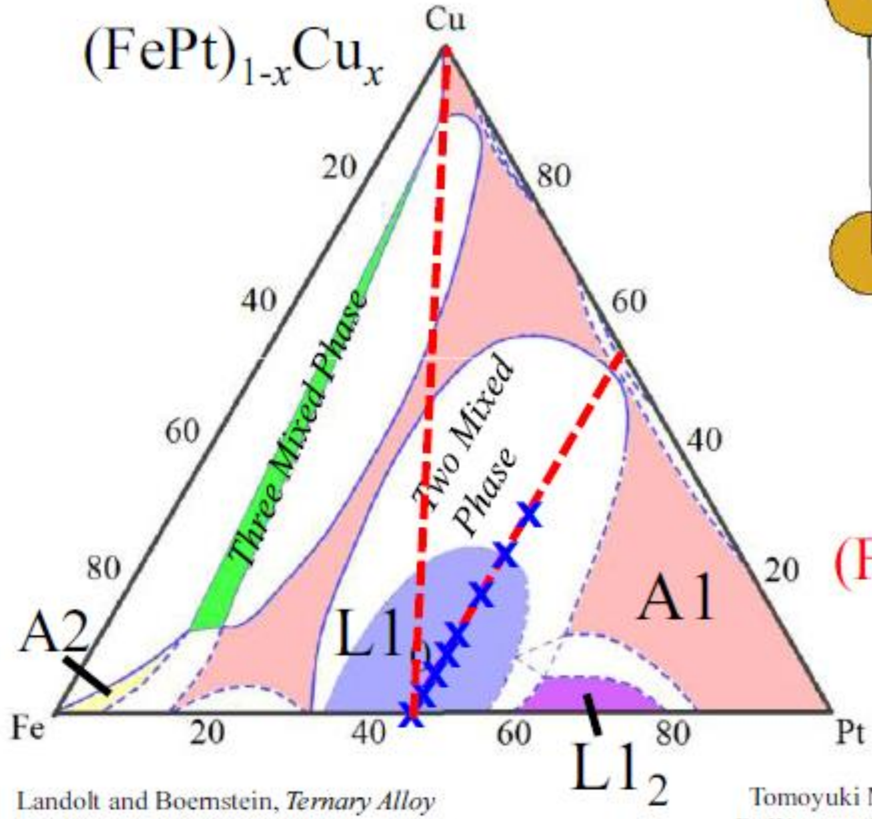

Landolt and Boernstein, *Ternary Alloy Systems*. (Springer-Verlag Berlin, 2008)

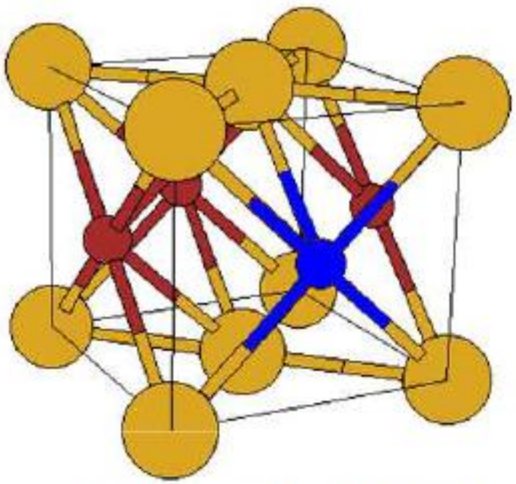

http://cst-www.nrl.navy.mil/lattice/index.html

Tomoyuki Maeda *et al.*, Appl. Phys. Lett. **80**, 2147 (2002)
B. Wang and K. Barmak, J. Appl. Phys. **109**, 123916 (2011)

UC Davis – Seagate

Composition dependence in Fe_xPt_{1-x}–C and $Fe_XCu_YPt_Z$

granular

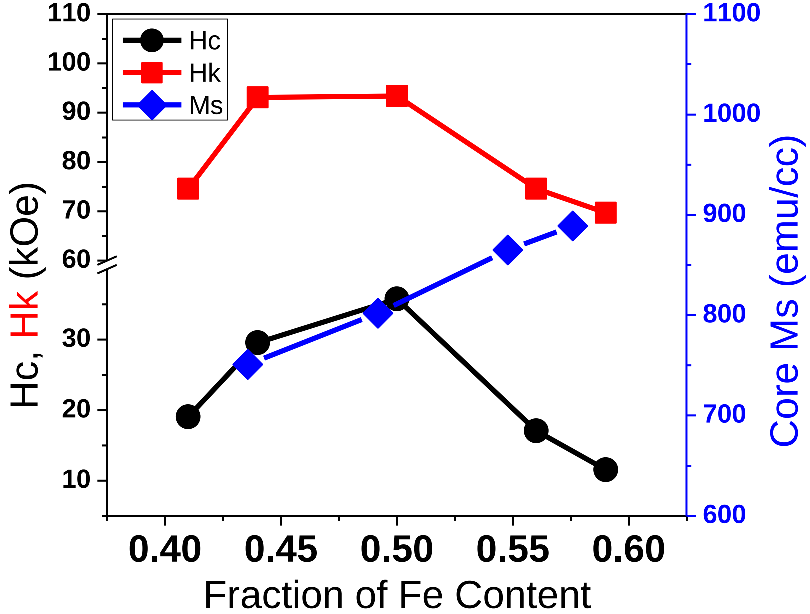

continuous

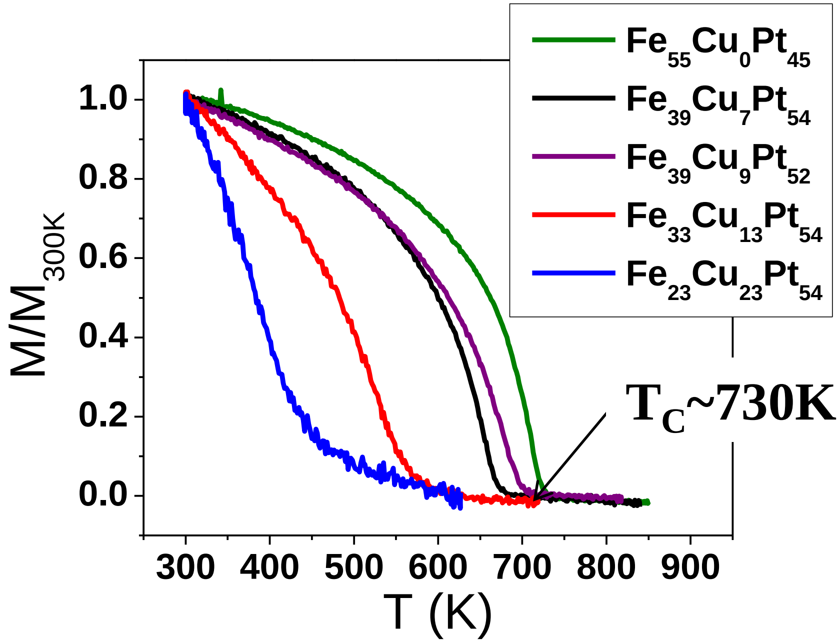

Optimal values of coercivity and anisotropy at x=50%

Curie temperature reduction to 600-650K by adding 9-13at% Cu

D. Weller et al., Phys. Status Solidi A 210, 1245 (2013)

FeCuPt IEEE SCV 11/19/13

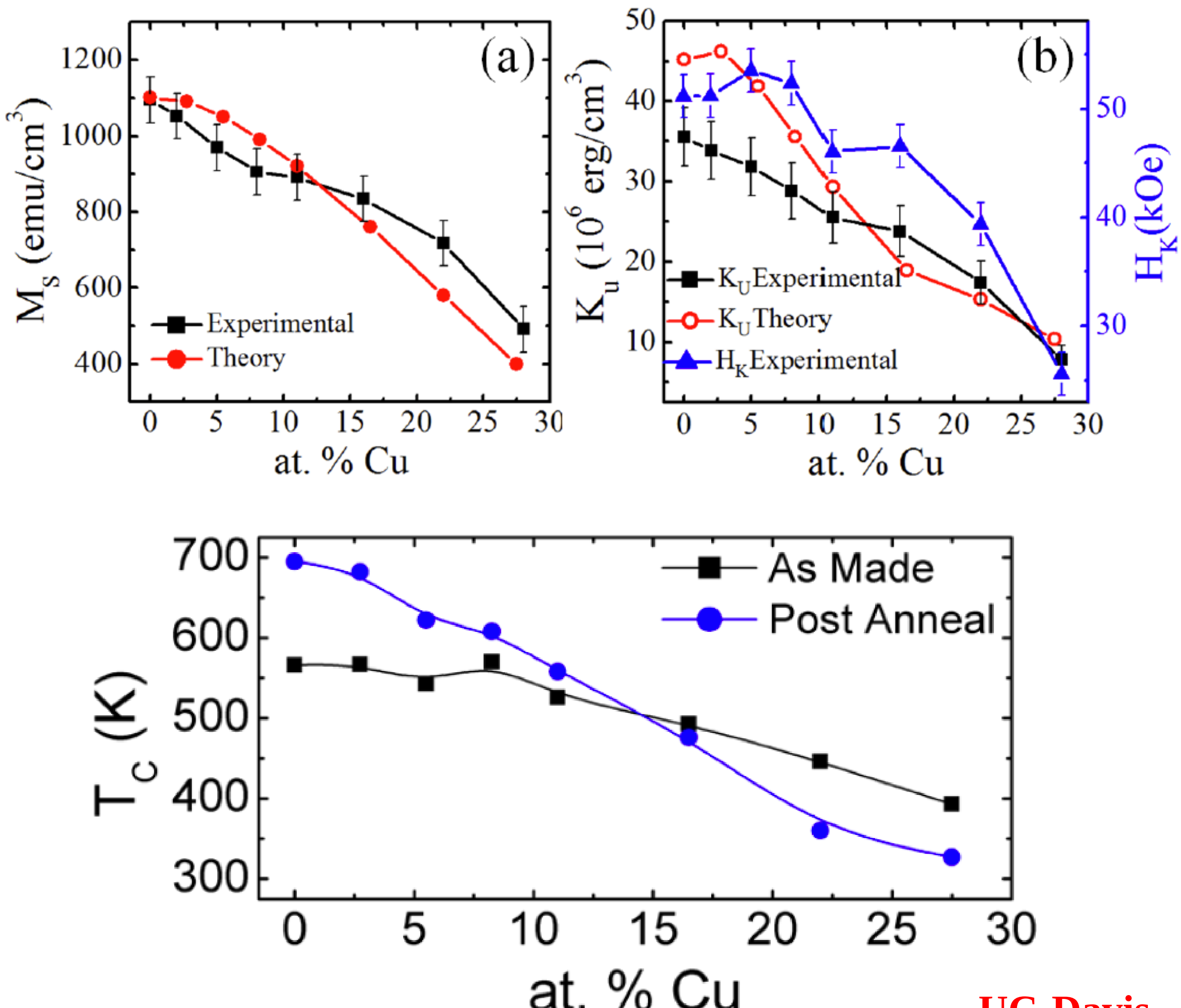

UC-Davis - Seagate

Grain Size and Microstructure from CoCrPt PMR to FePt HAMR 2013

Typical PMR

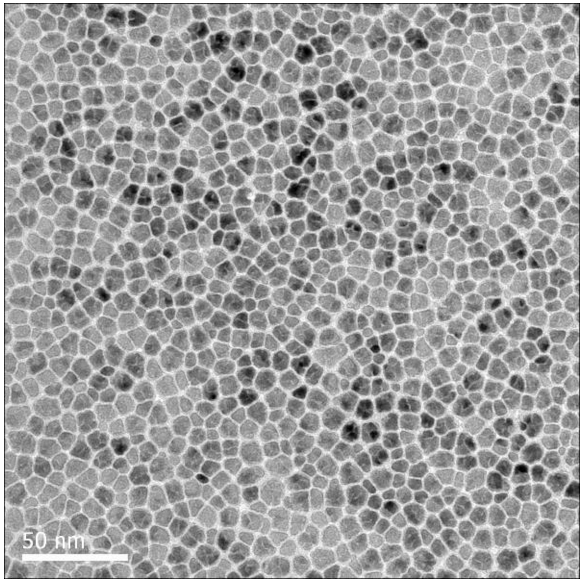

HAMR Media

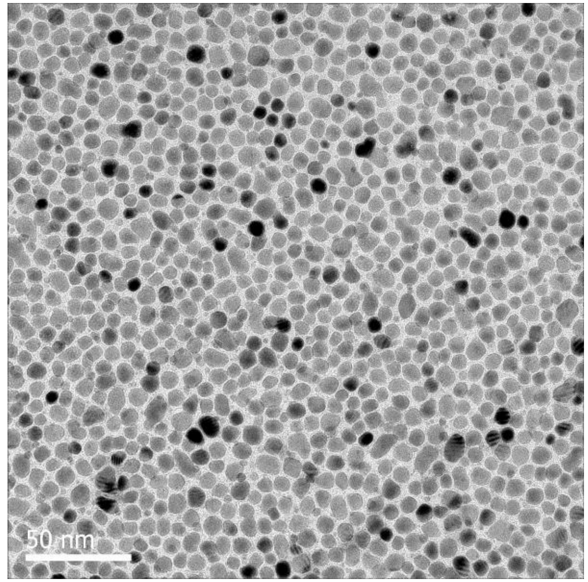

HAMR: more Voronoi and columnar

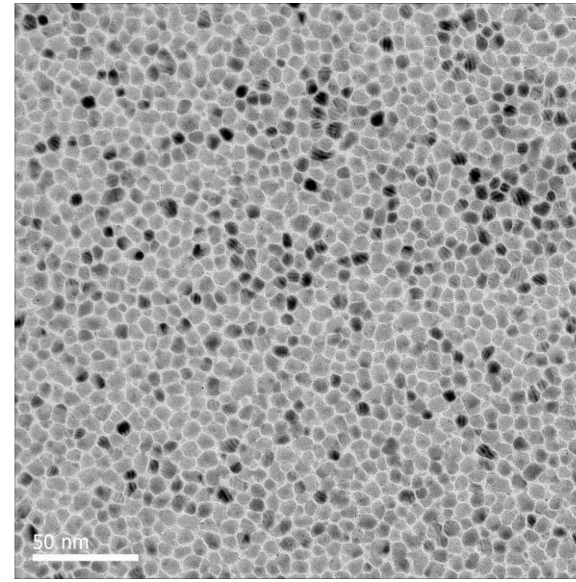

Improved Grain Size (Pitch) & Distributions